D I P L O M A R B E I T

Antenna Selection for MIMO Systems with Space-Time Coding

ausgeführt zum Zwecke der Erlangung des akademischen Grades eines Diplom-Ingenieurs
unter der Leitung von

Univ.Prof. Dipl.-Ing. Dr.techn. Johann Weinrichter
Dipl.-Ing. Biljana Badic
Institut für Nachrichtentechnik und Hochfrequenztechnik (E 389)

eingereicht an der Technischen Universität Wien
Fakultät für Elektrotechnik und Informationstechnik

von

Paul Fuxjäger

Matrikelnr.: 9426141
Rotenhofgasse 77/29
1100 Wien

Wien, Oktober 2004 . . . . . .

Kurzfassung

Der Einsatz von mehreren Antennen an beiden Enden eines Übertragungssystems ist unter dem Namen Multiple-Input Multiple-Output (MIMO) Technologie bekannt. Diese vielversprechende Methode eignet sich um die Kapazität und Empfangsqualität von Mobilfunksystemen signifikant zu steigern. Die technische Realisierung von MIMO Systemen wird jedoch unter anderem erschwert durch die hohe Anzahl an erforderlichen Hochfrequenz Ein- und Ausgangsstufen.

Antennen-Selektion ist eine attraktive Methode um diese Anforderung abzuschwächen. Hierbei wird nur eine Teilmenge aller vorhandenen Antennen verwendet und diese dem gegenwärtigen Kanalzustand optimal angepasst um die Leistungseinbußen im Vergleich mit dem ursprünglichen System so gering wie möglich zu halten.

Diese Diplomarbeit befasst sich mit MIMO-Übertragung mit Hilfe von Space-Time Block Codes (STBC) in Verbindung mit Antennen-Selektion. Der orthogonale Alamouti STBC sowie eine erweiterte quasi-orthogonale Variante davon werden im Detail studiert. Die System-Performance des quasi-orthogonalen Codes wird unter Verwendung eines linearen Zero-Forcing (ZF) Empfängers analysiert. Geschlossene, exakte Ausdrücke für die Bitfehlerhäufigkeit werden ermittelt und bilden die Basis für die Formulierung der optimalen Selektionskriterien im Falle des hier zu Grunde liegenden nichtfrequenzselektiven, quasi-statischen MIMO-Kanals.

Alle drei Varianten der Selektion (empfängerseitig, senderseitig und kombiniert) werden verglichen und die Endergebnisse der durchgeführten numerischen Simulationen dargestellt. Erreichbare Diversitätsgewinne, sowie Verbesserungen des mittleren Signal-zu-Geräusch Abstands am Empfänger werden abgeschätzt. Im Falle des quasi-orthogonalen STBCs werden die Ergebnisse, welche auf der Anwendung des optimale Kriteriums basieren den Resultaten für eine kleine Anzahl sub-optimaler Selektions-Algorithmen gegenübergestellt.

Es stellt sich heraus, dass sobald der verwendete STBC nicht mehr die Eigenschaft der vollständigen Orthogonalität besitzt, sich mit den einfachen

Selektions-Kriterien welche als optimal für orthogonale Codes gelten keine guten Ergebnisse mehr erzielen lassen.

Die Leistungsfähigkeit von Systemen mit Antennen-Selektion hängt stark von den statistischen Eigenschaften des benutzten MIMO Kanals ab. Dieser Umstand motivierte die Durchführung von zusätzlichen Simulationen, basierend auf einem einfachen stochastischen Kanal-Korrelationsmodell. Die dadurch gewonnenen Resultate erlauben die Abschätzung der Leistungseinbußen wenn der MIMO Kanal nicht mehr als unkorreliert angenommen werden kann.

Abstract

Multiple-Input multiple-output (MIMO) technology is capable of enhancing capacity and coverage of wireless links. Implementation of MIMO devices is intricate because of the increased number of radio frequency chains (one for each antenna element). Antenna selection is one attractive approach to mitigate this requirement. It only utilizes an optimal subset of all available antennas, adapting it to the current channel state in order to minimize the performance loss compared to the full complexity system.

This diploma thesis is dedicated to the analysis of space-time block coded MIMO transmission systems with antenna selection. The orthogonal Alamouti space-time block coding scheme as well as an extended non-orthogonal variant of it are studied in detail, the performance of the latter is evaluated using low-complexity linear zero-forcing receivers. The respective exact instantaneous bit error ratio expressions are acquired, providing the basis for the formulation of optimal selection criteria for the considered non-frequency selective, quasi-static MIMO channel.

All three possible variants namely receive, transmit and combined selection are compared to each other and the results of numerical simulations are presented. Achievable diversity gains as well as changes in average signal to noise ratio (SNR) at the receiver are given. For the case of the non-orthogonal space-time block coding scheme the performance figures using the optimal criterion are compared to the results for a given set of sub-optimal, generally less complex selection algorithms. It will be shown that the simple selection procedures that are able to maximize performance for orthogonal space-time block codes only deliver moderate selection gains when applied to non-orthogonal codes.

Obviously, the usability of antenna selection largely depends on the statistical characteristics of the MIMO channel. This motivated the execution of additional simulations using a simple stochastic channel-correlation model. The hereby obtained results allow to assess the performance deterioration when the MIMO channel is not spatially uncorrelated anymore.

Contents

Chapter 1

Introduction

Utilizing more than one antenna at both sides of the wireless communication link is known as MIMO (multiple-input, multiple-output). This technique promises significant enhancements of system performance without requiring the allocation of extra spectrum. Since the first analytic investigations [1, 2, 3] the scientific research in this field has made vast progress and MIMO is believed to be the key technology for future wireless standards.

Multiple antennas can be applied in various ways. A technique called spatial multiplexing seeks to enhance the spectrum efficiency by simultaneous transmission of independent data streams. This is done by turning multipath propagation, normally a handicap of mobile communication into a benefit for the system [4].

One alternative method called space-time coding [5, 6] improves the link reliability by introducing so called spatial diversity (also referred to as antenna diversity). A single data stream is encoded and the resulting signals transmitted from the multiple antenna elements are highly correlated. This redundancy in time *and* space enables the receiver to optimally combine the signal components picked up by the respective receive antennas [7].

While spatial multiplexing directly tries to improve the data-rate of the system, one can attain a similar benefit with the help of space-time coding. In a multipath fading situation the additional diversity increases the average quality of the received signal. Within given transmit-power constraints this can for instance be exploited by applying higher modulation formats, thus indirectly enhancing the achievable spectrum efficiency [8].

Generally, space-time codes can be divided into two classes. The first group is called space-time trellis codes (STTC) [6]. As the name implies their encoding procedure involves trellis stages to derive the transmit symbol streams. The incoming bits select the current state transition, every possible transition is then mapped onto a vector of transmit symbols whose

components are sent via the individual antennas [8]. This scheme offers diversity gain as well as additional coding gain but it also decreases the data rate since the total number of valid transmit signal vectors is lowered. Moreover, the decoding procedure requires a trellis search and its complexity grows exponentially with the number of used antennas and the length of the trellis.

The second category of space-time codes is based on block orientated processing [9, 10]. In the first trivial encoding step the bit sequence is mapped onto a symbol sequence. Subsequently, a block of successive symbols is linearly combined to a space-time coding matrix whose columns represent the symbol vectors transmitted via the individual antennas over time. Compared to their trellis-based counterparts these space-time block codes (STBC) are easier to decode but they do not exhibit any coding gain.

According to [11] the low-complexity feature of STBCs outweighs their lack of coding gain since concatenating them with simple additional outer codes can easily compensate for this without sacrificing much data rate. As a consequence this diploma thesis exclusively deals with the application of STBCs and in the following the motivation for the combination of space-time block coded MIMO transmission with antenna selection with is outlined.

The main challenge engineers are faced with when actually implementing MIMO devices is the increased complexity. This complexity stems from the following two facts.

1. **Increased processing effort.**
   Both transmitter and receiver need to be equipped with powerful signal-processors in order to handle the algorithmic intricacy introduced by the use of multiple antennas.

2. **Multiple radio-frequency (RF) front ends.**
   The *simultaneous* utilization of multiple antennas also implies that the number of costly analog-circuitry elements integrated on both sides of the link is significantly higher compared to the single antenna case.

Technical advancements in the field of digital signal processor (DSP) design are made significantly faster then in the domain of low cost integration of high frequency analog equipment. Consequently, the need for more DSP power will eventually become less of a problem. The following quote taken from [12] confirms this conjecture:

> "While additional antenna elements (patch or dipole antennas) are usually inexpensive, and the additional digital signal processing power becomes ever cheaper, the RF elements are expensive and do not follow Moore's law."

One attractive way to reduce the number of RF chains is antenna selection [13, 14, 15, 16]. Systems equipped with this capability optimally choose a subset of the available transmit and receive antennas and only process the signals associated with them. This allows to maximally benefit from the multiple antennas within given RF complexity and cost constraints.

Obviously, the performance penalties compared to the non-selective, full complexity system primarily depend on the capability of the applied selection algorithm to compute the subset that is best suited (optimum) for the current channel state.

This thesis is dedicated to the analysis of the performance of various antenna selection algorithms in a space-time block coding context. For a given set of codes the optimum selection criteria, minimizing the instant bit error ratio (BER) will be formulated. Using numerical Monte-Carlo simulations written in MATLAB[1] the resulting system performances are evaluated and compared. These comparisons will also partly incorporate performance results for non-selective systems.

Generally, using space-time block coding, the performance of antenna selection systems can be related to that of non-selective systems in two different ways:

1. **Direct comparison with the full complexity system.**
   In case of transmit selection this implies that different underlying space-time codes are applied in the full complexity system since it uses all of the available antennas simultaneously. So the differences in performance cannot be attributed to the antenna-selection alone.

2. **Comparison with the same non-selective setup.**
   Here setups with selection capability are compared to their counterparts that do not incorporate any antenna selection at all but use the exact same space-time block code.

The latter point of view also corresponds to an approach where a given system is to be improved via the addition of inexpensive antenna elements and switches needed for antenna selection. It offers a simple and economical way to enhance the performance of any given wireless communication equipment.

All three possible variants of antenna selection are analyzed in this thesis:

1. Antenna selection at the receiver only

[1] Copyright TheMathworks Inc.

2. Antenna selection at the transmitter only

3. Antenna selection at both ends

whereas the last variant is treated only marginally since the main focus has been set on working out the differences between receive and transmit selection.

In all of those selection scenarios the computation of the optimum antenna subset is based on estimates of the channel coefficients as perceived by the receiver. Since channel reciprocity can not be assumed in general the transmitter cannot do this by itself and needs to be provided with that subset information. This critical requirement is a major drawback of transmit and combined selection schemes. Furthermore, the information rates of permanently available feedback links are usually very limited. It is therefore of interest to devise closed loop schemes that can achieve high selection gains with as little feedback information as possible. This aspect is addressed in every chapter involving closed loop antenna selection.

1.1 Outline

The diploma thesis is organized as follows:

Chapter 2 defines the used system model. In order to set the scope of this thesis some important simplifications have to be made. The attributes of the considered channel model are defined rigorously. All the subsequent chapters refer to the assumptions presented in this preface.

Chapter 3 gives the first introduction into the field of antenna selection. The performance of a simple non-space-time coded system is observed in combination with receive and transmit selection. Additionally two possible methods of estimating the diversity gain on the basis of numerical simulation results are analyzed.

Chapter 4 introduces the well known Alamouti transmission scheme. The optimum selection criterion is worked out and further generalized to arbitrary orthogonal space-time block codes. The presentation of simulation results constitutes the remainder of this chapter.

Chapter 5 presents an extended variant of the Alamouti scheme that uses four transmit antennas simultaneously. Due to its non-orthogonality the selection strategies presented in the previous chapter need to be adapted.

Simulations are used to document the performance differences between the obtained optimum and several sub-optimum selection algorithms.

Chapter 6 compares the results from the preceding chapters and tries to give a compact summary over all conducted simulations.

Chapter 2

System Model

The following sections define the system model that has been used in the simulations presented in this work. They also frame the scope of this thesis because they clearly specify which elements of the communication system are take into consideration. Hence, the presented simplifying assumptions had to be made in order to reduce the problem-complexity, some of them were specifically adapted to facilitate comparisons with the contributions of other authors.

Throughout this thesis the following notation is used:

N_t	Total number of available transmit antennas.
n_t	Number of selected transmit antennas.
N_r	Total number of available receive antennas.
n_r	Number of selected receive antennas.

Thus, a specific antenna selection scheme is identified by the quadruple (N_t,n_t,N_r,n_r), whereas the underlying STBC scheme will be denoted as a ($n_t \times n_r$) space-time coding architecture.

2.1 Communication Setup

Figure 2.1 depicts the structure of the considered MIMO-STBC transmitter. It features antenna selection capability and consists of the following three stages:

1. **STBC coding unit**
   This device maps the bits of the input data stream b_k to symbols and subsequently forms the space-time block matrix whose columns constitute the resulting n_t symbol streams.

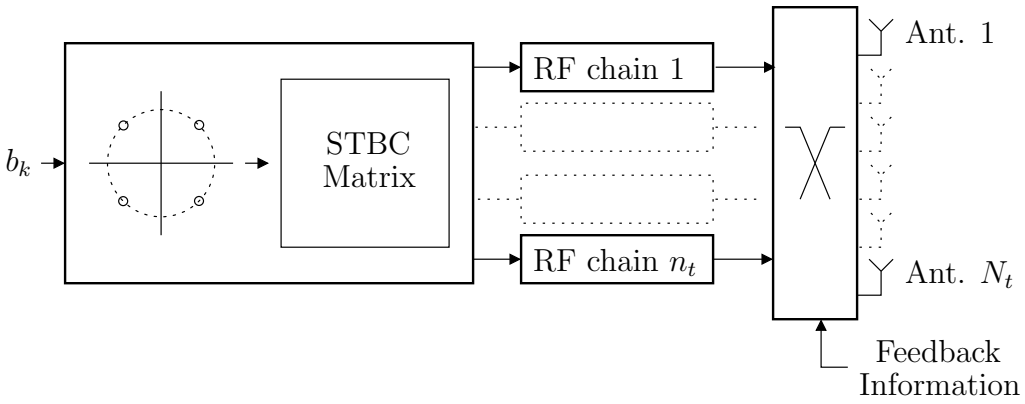

Figure 2.1: MIMO-STBC transmitter with antenna selection

2. **Radio-Frequency chains**
   These entities convert the n_t symbol streams from the digital baseband domain to analog radio-frequency. Thus *each* RF-chain must at least have one of the following elements implemented:

   - Digital/analog converter
   - Mixer
   - Power amplifier
   - Additional analog circuitry (filters, impedance converters, ...)

   Note that some of the required analog components do not have to be replicated necessarily for each RF-path since their functionality could be reused (e.g. the local oscillators).

3. **Antenna-selection switch**
   This switch is controlled by the selection logic located at the receiver via the feedback information link and connects the outputs of the RF-chains to n_t of the total available N_t transmit antenna elements.

The structure of the receiver presented in Figure 2.2 is similar to the reverse structure of the transmitter. The receive selection switch connects n_r out of N_r antennas to the RF down-conversion chains. Synchronization equipment follows and the respective signal streams are fed to the space-time decoder together with estimates of the channel coefficients. Symbol decision and final symbol-to-bit mapping terminates the communication process. The estimated channel coefficients are also relayed to the antenna selection logic in order to be able to compute the appropriate antenna subsets for both sides

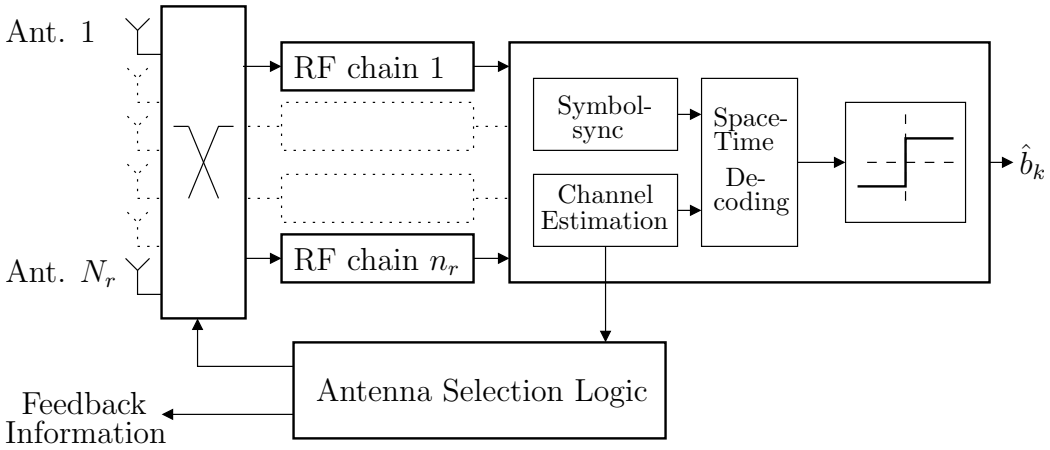

Figure 2.2: MIMO-STBC receiver with antenna selection

of the link.

In this thesis only functional aspects of the channel, the space-time coding and decoding schemes as well as the antenna selection algorithms are taken into consideration. All the remaining parts in the signal chain are treated like ideally operating components.

This results in the following assumptions:

- **Linearity**
  No distortion is introduced by the analog up- and down-conversion units and no crosstalk between these RF-chains is present.
- **Synchronization**
  Perfect synchronization is given for all times.
- **Channel Estimation**
  Perfect channel state information (CSI) is present at the receiver. No channel estimation errors are made.
- **Ideal Switching**
  The switches performing the actual antenna selection are seen as elements with identical, linear transfer characteristics associated with the respective input-output pairs. They are assumed to introduce no insertion loss.

- **Feedback Link Properties**
  The feedback link has no latency, thus the antenna subset information is instantly available at the transmitter. Furthermore, this communication link is assumed to be absolutely free of transmission errors.

2.2 Channel Model

The wireless channel is considered non-frequency selective. Thus every instant channel realization is characterized by a single complex number in the SISO (2.1) setup, a row vector of complex numbers in the MISO (2.2) case, a column vector of complex numbers in the SIMO (2.3) case and a complex two-dimensional matrix for MIMO (2.4) considerations.

In (2.4) the first index of the elements h_{ij} refers to the respective receive antenna, the second index identifies the associated transmit antenna.

$$h_{\text{SISO}} = h \ , \tag{2.1}$$

$$\mathbf{h}_{\text{MISO}} = \begin{bmatrix} h_1 & h_2 & \dots & h_{N_t} \end{bmatrix} \ , \tag{2.2}$$

$$\mathbf{h}_{\text{SIMO}} = \begin{bmatrix} h_1 \\ h_2 \\ \vdots \\ h_{N_r} \end{bmatrix} \ , \tag{2.3}$$

$$\mathbf{H}_{\text{MIMO}} = \begin{bmatrix} h_{11} & h_{12} & \dots & h_{1N_t} \\ h_{21} & h_{22} & \dots & h_{2N_t} \\ \vdots & \vdots & \ddots & \vdots \\ h_{N_r1} & h_{N_r2} & \dots & h_{N_rN_t} \end{bmatrix} \ . \tag{2.4}$$

The time-dependent statistical properties are defined according to the **block fading** definition [8]. Thus for L_s successive symbol cycles the instant channel realization, given by one of (2.1) - (2.4) is considered fixed. At block boundaries a completely new realization is randomly generated with no statistical relation to the previous channels. This model is also referred to as **quasi-static**.

The probability density functions (pdfs) of the channel coefficients are kept constant over all blocks, i.e the same pdfs are realized for the whole duration of the transmission (c.f. Section 2.2.1).

In all numerical calculations presented the blocklength value is kept constant at $L_s = 2048$ symbol cycles. However, due to the quasi-static channel assumption the blocklength can be chosen arbitrarily *without* effecting the results. The following remarks illustrate this implication:

A complete simulation run consists of several independent sub-simulations for different values of signal-to-noise ratio (SNR). At the end of each sub-simulation the average bit error ratio (BER) for the current SNR value is calculated by dividing the number of incorrectly detected bits by the total number of transmitted bits:

$$\overline{\mathrm{BER}} = \frac{1}{N\,L_b} \sum_{k=1}^{N} b_{err,k} \tag{2.5}$$

with N being the number of simulated blocks (equalling the number of simulated channel instances). Hence, during each block k, the same number of L_b bits are transmitted, with $b_{err,k}$ bits being erroneous.

L_b is directly related to the blocklength L_s via: $L_b = L_s \log_2(M_a)$, with M_a being the size of the utilized symbol alphabet (see Section 2.3). Thus M_a equals 4 and $L_b = 8192$.

Now let the *instantaneous* bit error ratio as a function of the current channel state be denoted by BER_k. Per definition, this quantity does *not* depend on the number of simulated bits per channel instance. Thus, the bit-errors occurring during the simulation of a given channel state can be assumed to be proportional to the number of transmitted bits:

$$b_{err,k} = \mathrm{BER}_k\, L_b\ . \tag{2.6}$$

From (2.5) and (2.6) follows:

$$\overline{\mathrm{BER}} = \frac{1}{N} \sum_{n=1}^{N} \mathrm{BER}_k\ . \tag{2.7}$$

Although BER_k is not directly available during the simulation the equivalence of (2.5) and (2.7) justifies the conclusion that the chosen value for L_b does not influence the respective end results.

To sum up, the irrelevance of the blocklength is due to the block-fading assumption and the resulting simulation scheme. As long as the variance of $\mathrm{BER_k}$ (depending on the statistical properties of the channel coefficients) is

taken care of by averaging over a large enough number of channel realizations the results will not be influenced by the chosen blocklength.

However, for more realistic non-quasi-static channel environments the blocklength is a critical parameter: Channel estimation and antenna selection is done at the beginning of each block only, choosing a very large value for L_s prevents the system to adapt to fast temporal changes of the channel. Conversely, decreasing the blocklength to a very small number corresponds to a high rate of required channel estimations and feedback transmissions. To sum up, in cases where more complex channel models are applied the blocklength needs to be adapted to the speed of temporal channel variations (e.g. observing the coherence time [18]).

2.2.1 Statistical Properties

Two different channel setups are distinguished:

1. No correlated between channel coefficients
2. Stochastically modelled correlation between channel coefficients

In the remainder of this thesis uncorrelated channels are simply denoted by $\mathbf{h}$ or $\mathbf{H}$, dropping the indices from (2.1) - (2.4), whereas correlated channels are referenced as $\mathbf{h}_{\text{corr}}$ or $\mathbf{H}_{\text{corr}}$ respectively.

Uncorrelated Channels

For any i, j the complex path gains $h_{i,j}$ are independently identically distributed (i.i.d). The pdf will now be elaborated in detail (the indices i, j are neglected in the following to keep the notation less bloated).

Real and imaginary parts of h are modelled as i.i.d. real valued gaussian random variables with zero mean:

$$h \triangleq X + jY \ .$$

Thus, the pdfs of X and Y are given by [23]:

$$pdf_X(\xi) = \frac{1}{\sqrt{2\pi}\sigma} \exp \frac{-\xi^2}{2\sigma^2} \qquad \xi \in \mathbb{R} \ , \tag{2.8}$$

$$pdf_Y(\zeta) = \frac{1}{\sqrt{2\pi}\sigma} \exp \frac{-\zeta^2}{2\sigma^2} \qquad \zeta \in \mathbb{R} \ . \tag{2.9}$$

Since both random variables are statistically independent and zero mean the mean and variance of h work out to

$$\mu_h = \mathrm{E}_k\{X\} + j\mathrm{E}_k\{Y\} = 0 \quad , \quad \sigma_h^2 = \mathrm{E}_k\left\{X^2\right\} + \mathrm{E}_k\left\{Y^2\right\} = 2\sigma^2 \ .$$

Here the expectation is meant with respect to the channel realizations k. The papers cited in this thesis define the channel coefficients to have variance $\sigma_h^2 = 1$, so in order to comply with these assumptions the variance of X and Y was accordingly chosen as $\sigma^2 = 0.5$.

An additional conclusion from statistical independent and zero mean X and Y is that $|h|^2 = X^2 + Y^2$ is central chi-squared distributed with two degrees of freedom [19]:

$$pdf_{|h|^2}(\alpha) = \frac{1}{2\sigma^2} \exp \frac{-\alpha}{2\sigma^2} \quad , \quad 0 \leq \alpha \; . \tag{2.10}$$

Furthermore, $|h|$ follows a Rayleigh distribution:

$$pdf_{|h|}(\beta) = \frac{\beta}{\sigma^2} \exp \frac{-\beta^2}{2\sigma^2} \quad , \quad 0 \leq \beta \; . \tag{2.11}$$

The variance of the chi-squared distribution (2.10) is related to the variance of X and Y by:

$$\sigma_{|h|^2}^2 = 4\sigma^4 = 1$$

and the variance of the Rayleigh distributed $|h|$ in (2.11) works out to:

$$\sigma_{|h|}^2 = (2 - \frac{1}{2}\pi)\sigma^2 \cong 0.2146 \; .$$

The means of $|h|^2$ and $|h|$ are given by:

$$\mu_{|h|^2}^2 = 2\sigma^2 = 1 \quad , \quad \mu_{|h|}^2 = \sqrt{\frac{\pi}{2}}\sigma \cong 0.8862$$

and finally, the phase of h is uniformly distributed:

$$pdf_{\psi(h)}(\gamma) = \frac{1}{2\pi} \quad , \quad -\pi \leq \gamma < \pi \; .$$

Figure 2.3 shows the histogram of $|h|$ for a set of 10^5 randomly generated complex values of h that were used in one of the simulations. Additionally the pdf of the corresponding Rayleigh distribution is drawn as a reference. For additional verification if the random number generation algorithms utilized in MATLAB are capable of producing i.i.d (i.e. uncorrelated) MIMO matrices the following short analysis was made:

A set of matrices $\mathbf{H}_k \in \mathbb{C}^{2\times 2}$ with $k = 1 \ldots 10^5$ was generated and the spatial correlation among this set was computed according to [20]:

$$\mathbf{R} = \mathrm{E}_k \left\{ \mathrm{vec}(\mathbf{H}_k) \mathrm{vec}(\mathbf{H}_k)^H \right\} \; , \tag{2.12}$$

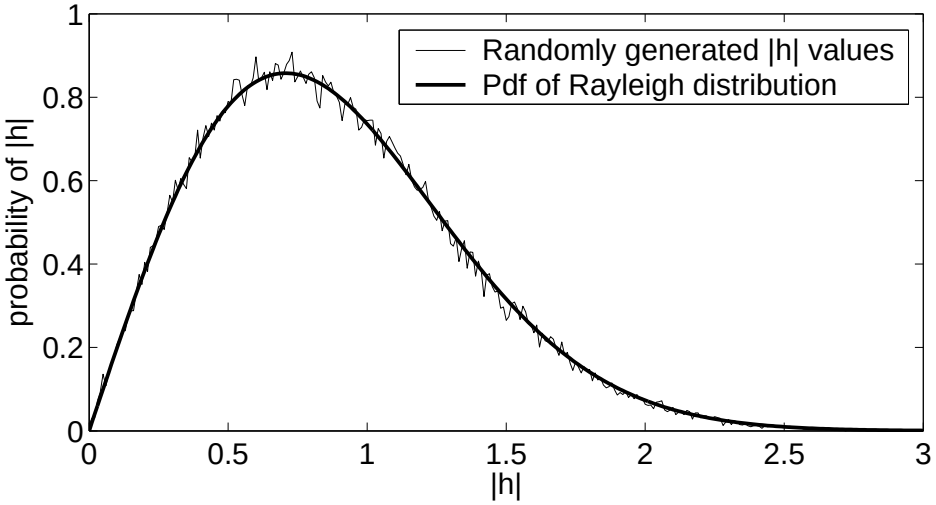

Figure 2.3: Histogram of $|h|$ for 10^5 generated channel values and the pdf of the corresponding Rayleigh distribution.

with $\mathbf{R} \in \mathbb{C}^{4\times4}$. The used vectorization operator stacks the columns of $\mathbf{H}_k$ in a single 4×1 vector. The absolute of the resulting correlation matrix is presented by (2.13). The very slight deviation from an 4×4 identity matrix is due to residual statistical dependencies between the outcomes of successive calls of the utilized `randn` algorithm in MATLAB.

$$|\mathbf{R}| = \begin{bmatrix} 0.9968 & 0.0018 & 0.0019 & 0.0033 \\ 0.0018 & 0.9991 & 0.0038 & 0.0033 \\ 0.0019 & 0.0038 & 0.9980 & 0.0032 \\ 0.0033 & 0.0033 & 0.0032 & 1.0053 \end{bmatrix} \tag{2.13}$$

Correlated Channels

Totally uncorrelated channel path gains are a highly unrealistic assumption. Existing MIMO channels exhibit spatial correlation resulting from the specific physical structure of the wave propagation space (i.e location and characteristics of antenna elements and scattering objects) [18]. This results in a MIMO channel matrix with significant statistical dependencies between its coefficients h_{ij}.

A simple stochastical method of introducing spatial correlation is extending the i.i.d case by means of multiplication with a suitably chosen correlation matrix [21]:

$$\text{vec}\{\mathbf{H}_{\text{corr}}\} = (\mathbf{R})^{\frac{1}{2}}\text{vec}\{\mathbf{H}\} \tag{2.14}$$

with $(\cdot)^{\frac{1}{2}}$ being defined as the matrix square root:

$$(\mathbf{R})^{\frac{1}{2}}[(\mathbf{R})^{\frac{1}{2}}]^H = \mathbf{R} \; .$$

By applying (2.14) the specific correlation characteristics of an existing MIMO channel can now be assigned onto $\mathbf{H}_{\text{corr}}$ by inserting the appropriate matrix $\mathbf{R}$. For instance, (2.12) provides a possible procedure to extract this correlation matrix from a set of measured channels. However, the simulations involving correlated channels presented in this paper are not based on specifically measured channels. Instead the correlation matrix $\mathbf{R}$ is synthesized as follows.

As a starting point the total channel correlation matrix $\mathbf{R}$ is assumed to be well approximated by the Kronecker product of two separate correlation matrices [20]:

$$\mathbf{R} = \frac{1}{\text{tr}\{\mathbf{R}_\text{r}\}} \mathbf{R}_\text{t}{}^T \otimes \mathbf{R}_\text{r} \; , \quad \mathbf{R} \in \mathbb{C}^{N_t N_r \times N_t N_r} \; . \tag{2.15}$$

Here, $\mathbf{R}_\text{t}$ and $\mathbf{R}_\text{r}$ specify the spatial correlation at the trasmitter side and the receiver side independently and they again can be computed from a given set of measured channels $\mathbf{H}_k$ via:

$$\mathbf{R}_\text{t} = \text{E}_k \left\{ \mathbf{H}_k^H \mathbf{H}_k \right\} \; , \quad \mathbf{R}_\text{r} \in \mathbb{C}^{N_r \times N_r} \; ,$$

$$\mathbf{R}_\text{r} = \text{E}_k \left\{ \mathbf{H}_k \mathbf{H}_k^H \right\} \; , \quad \mathbf{R}_\text{t} \in \mathbb{C}^{N_t \times N_t} \; .$$

Equation (2.15) is generally referred to as the Kronecker model [21] and by using the identity

$$[\mathbf{B}^T \otimes \mathbf{A}]\text{vec}\{\mathbf{D}\} = \text{vec}\{\mathbf{ADB}\}$$

together with (2.14) and (2.15) the following equation is obtained:

$$\mathbf{H}_{\text{corr}} = \frac{1}{\sqrt{\text{tr}\{\mathbf{R}_\text{r}\}}} (\mathbf{R}_\text{r})^{\frac{1}{2}} \mathbf{H} [(\mathbf{R}_\text{t})^{\frac{1}{2}}]^T \; . \tag{2.16}$$

The accuracy of (2.16) has been demonstrated in [20] for non-frequency selective channels in NLOS (non-line-of-sight) indoor environments.

Finally, the Kronecker model was applied using the following specifically structured correlation matrices $\mathbf{R}_\text{t}$ and $\mathbf{R}_\text{r}$:

$$\mathbf{R}_\text{t} = \mathbf{R}_\text{t}^T = \begin{bmatrix} 1 & \rho_\text{t} & \rho_\text{t}^2 & \dots & \rho_\text{t}^{N_r-1} \\ \rho_\text{t} & 1 & \rho_\text{t} & \dots & \rho_\text{t}^{N_r-2} \\ \rho_\text{t}^2 & \rho_\text{t} & 1 & \dots & \rho_\text{t}^{N_r-3} \\ \vdots & \vdots & \vdots & \ddots & \vdots \\ \rho_\text{t}^{N_r-1} & \rho_\text{t}^{N_r-2} & \rho_\text{t}^{N_r-3} & \dots & 1 \end{bmatrix} \; , \tag{2.17}$$

$$\mathbf{R}_{\mathrm{r}} = \mathbf{R}_{\mathrm{r}}^{T} = \begin{bmatrix} 1 & \rho_{\mathrm{r}} & \rho_{\mathrm{r}}^{2} & \dots & \rho_{\mathrm{r}}^{N_r-1} \\ \rho_{\mathrm{r}} & 1 & \rho_{\mathrm{r}} & \dots & \rho_{\mathrm{r}}^{N_r-2} \\ \rho_{\mathrm{r}}^{2} & \rho_{\mathrm{r}} & 1 & \dots & \rho_{\mathrm{r}}^{N_r-3} \\ \vdots & \vdots & \vdots & \ddots & \vdots \\ \rho_{\mathrm{r}}^{N_r-1} & \rho_{\mathrm{r}}^{N_r-2} & \rho_{\mathrm{r}}^{N_r-3} & \dots & 1 \end{bmatrix} , \tag{2.18}$$

with real valued correlation coefficients:

$$\rho_{\mathrm{t}}, \rho_{\mathrm{r}} \in \mathbb{R} , \quad 0 \leq \rho_{\mathrm{t}}, \rho_{\mathrm{r}} \leq 1 .$$

These Toeplitz structured matrices are appropriate for modelling the statistical behavior when the antenna elements at the transmitter as well as at the receiver are collocated linearly [22].

When applying the synthetic correlation matrices given by (2.17) and (2.18) the normalization factor in (2.16) needs to be omitted, resulting in:

$$\mathbf{H}_{\mathrm{corr}} = (\mathbf{R}_{\mathrm{r}})^{\frac{1}{2}} \mathbf{H} [(\mathbf{R}_{\mathrm{t}})^{\frac{1}{2}}]^{T} \tag{2.19}$$

because otherwise the equivalent SISO power channel factor γ given by:

$$\gamma = \mathrm{E}_k \left\{ \frac{1}{N_r N_t} \sum_{i}^{N_r} \sum_{j}^{N_t} |h_{ij}|^2 \right\}$$

would not be equal for both $\mathbf{H}_{\mathrm{corr}}$ and $\mathbf{H}$. A change of γ would result in a change of the average receive SNR which is not intended when introducing channel correlation.

To sum up, using this specific modelling approach results in the following dependencies between h_{ij}. The coefficients corresponding to adjacent transmit antennas are correlated according to:

$$\mathrm{E}_k \left\{ h_{i,j}\, h_{i,j+1}^{*} \right\} = \rho_{\mathrm{t}} , \quad j \in \{1 \dots N_t - 1\} \tag{2.20}$$

independent from the respective receive antenna i. Analogously the dependency of adjacent receive antenna channel coefficients is given by:

$$\mathrm{E}_k \left\{ h_{i,j}\, h_{i+1,j}^{*} \right\} = \rho_{\mathrm{r}} , \quad j \in \{1 \dots N_r - 1\} \tag{2.21}$$

and does not depend on the transmit antenna index j.

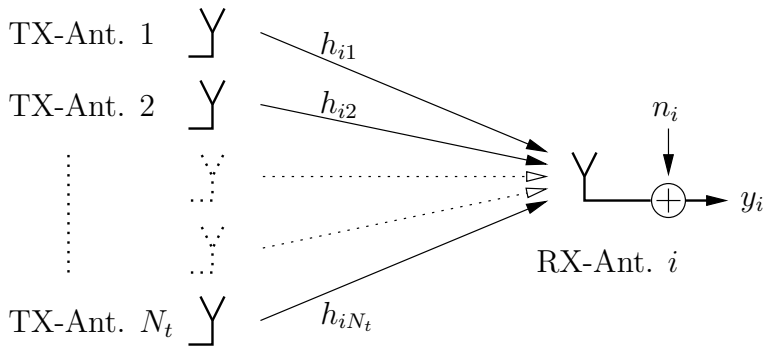

Figure 2.4: Linear superposition of transmit-symbols at antenna i

2.3 Signal Representation

The total signal path ranging from the output of the space-time coder to the input of the decoder can be represented by an equivalent discrete time baseband MIMO channel. This is justified by the assumptions made in Sections 2.1 and 2.2 and the transmit signals are henceforth only represented by the respective transmit symbols. The received signals result in a linear combination of the transmit symbols (weighted by the channel path gains h_{ij}) perturbed by additive complex gaussian noise. During any given symbol cycle the received signal at antenna i is obtained as:

$$y_i = \sum_{j}^{N_t} h_{ij} s_j + n_i \; . \tag{2.22}$$

This relation is depicted in Figure 2.4. Obviously (2.22) is conveniently expressed in vector matrix notation:

$$\mathbf{y} = \mathbf{H}\mathbf{s} + \mathbf{n} \tag{2.23}$$

with the already defined MIMO channel matrix (2.4):

$$\mathbf{H} = \begin{bmatrix} h_{11} & h_{12} & \dots & h_{1N_t} \\ h_{21} & h_{22} & \dots & h_{2N_t} \\ \vdots & \vdots & \ddots & \vdots \\ h_{N_r1} & h_{N_r2} & \dots & h_{N_rN_t} \end{bmatrix} \tag{2.24}$$

and the column vectors for the transmit, receive and noise signals:

$$\mathbf{s} = \begin{bmatrix} s_1 \\ s_2 \\ \vdots \\ s_{N_t} \end{bmatrix}, \quad \mathbf{y} = \begin{bmatrix} y_1 \\ y_2 \\ \vdots \\ y_{N_r} \end{bmatrix}, \quad \mathbf{n} = \begin{bmatrix} n_1 \\ n_2 \\ \vdots \\ n_{N_r} \end{bmatrix} . \tag{2.25}$$

Note that no antenna selection has been applied yet, all transmit and receive antennas are considered active in (2.23) - (2.25).

Noise

According to (2.22) the received signal is only corrupted by additive noise. These noise samples are modelled as i.i.d zero mean complex gaussian random variables. Thus the pdfs for real and imaginary part are equal to the ones given by (2.8) and (2.9) with variance $\sigma^2 = \frac{1}{2}\sigma_n^2$ instead.

Again, zero mean and statistical independence of real and imaginary part results in a total variance (equalling the power of the discrete-time complex noise) of:

$$\sigma_n^2 = N_0 \, . \tag{2.26}$$

Additionally, the noise samples present at different receive antennas are assumed to be statistically independent which results in:

$$\mathrm{E}\left\{\mathbf{n}\,\mathbf{n}^H\right\} = \sigma_n^2 \mathbf{I}_{N_r} \, . \tag{2.27}$$

In the above equation the expectation is taken over the discrete symbol time instants and $\mathbf{I}_{N_r}$ denotes the $N_r \times N_r$ identity matrix.

Symbol Constellation

The utilized quadrature phase shift keying (QPSK)[1] symbol alphabet is depicted in Figure 2.5. This constellation consists of four symbols each having two nearest neighbors. They are located on a square lattice and the error-probabilities for the additive white gaussian noise (AWGN) case are therefore easy to compute.

$$s \in \{1 + j, -1 + j, -1 - j, 1 - j\} \tag{2.28}$$

It is worth noting that sign inversion and/or complex conjugation of a QPSK symbol results in another valid QPSK symbol. Since the analyzed STBC

[1] equivalent to 4-QAM (Quadrature Amplitude Modulation)

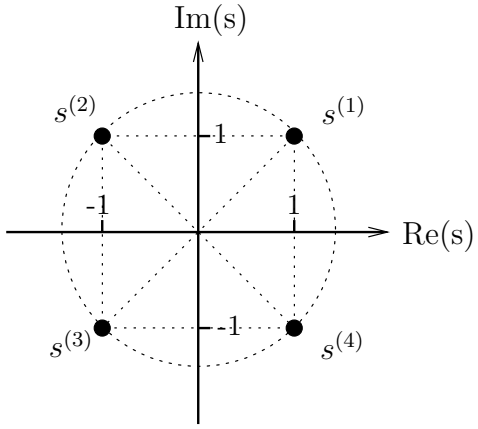

Figure 2.5: Used QPSK symbol constellation

mutually use these two operations to form entries of the space-time block matrix this property may be of relevance. However, it can be shown that this aspect is only of importance for non-linear receivers such as the maximum likelihood (ML) detector which is not discussed in in this thesis.

The to be transmitted bit-sequence is modelled as a stationary white random process, yielding equally likely and statistically independent symbols and finally, the bit-to-symbol mapping is defined obeying a Gray code rule [23], to ensure that a nearest neighbor symbol error only results in a single bit transmission error.

2.4 Normalization Issues

The simulation results are presented by plotting the average BER over $\frac{E_b}{N_0}$ in double logarithmic scaling. The quotient $\frac{E_b}{N_0}$ does not directly relate to a receive SNR. This is an important notational difference to the results presented by other authors, where E_b is related to the average bit energy at the receiver. Instead, the following rule is assumed:

E_b references the average energy per transmitted bit, emitted by the sum of all active transmit antennas per discrete symbol cycle.

This alternative transmit-energy based normalization has been chosen due to the nature of the simulated antenna selection setup. A receive-SNR based normalization would eliminate the possibility to compare different closed loop simulations. To illustrate this case consider a scheme that has the ability of selecting the optimum (by an arbitrary criterion) transmit antenna out of

N_t available ones. The average receive SNR for this scheme is considerably higher than for the case where no transmit selection is done. Thus plotting the average BER over $\frac{E_b}{N_0}$ with E_b being the average energy per bit at the receiver would subtract any transmit selection gain from the results.

It is therefore recommended to normalize the results by referencing them to a quotient of transmit bit energy and receiver noise.

Since no multi-user aspects are considered two dual approaches are applicable to simulate different values of $\frac{E_b}{N_0}$:

- Transmit-power variation
- Noise-power variation

In the presented simulations the latter is used and the simulated values of $\frac{E_b}{N_0}$ range form -5...20 [dB].

2.5 Feedback Issues

As mentioned in Section 2.1 every closed loop scheme (transmit and combined selection) requires the transmitter to be informed of the transmit antenna subset for the current channel realization. The next few paragraphs will elaborate on the question of how to quantify the minimum number of bits necessary for the transmission of this information.

In this thesis, instead of transferring the indices of the selected antennas separately, all effectively different subsets are numbered and only the corresponding subset-index number is fed back.

Note the significant difference between the number of *possible* and the number of *effectively different* subsets. Since the transmit selection switch is also capable of swapping the order of utilized antennas (e.g. first row of space-time code matrix gets transmitted via antenna two and vice versa) the first term corresponds to all possible combinations of n_t out of N_t elements while observing order:

$$q = \frac{N_t!}{(N_t - n_t)!} = n_t! \binom{N_t}{n_t} \tag{2.29}$$

The second quantity of effectively different subsets is in many cases substantially lower, depending on the applied space-time coding scheme.

In this context effectively different means that the respective subsets produce different results at the output of the space-time decoder. Consider a

space-time block coding scheme where the permutation of antennas inside the chosen subset does not change the outcome of the transmission at all. This would be the case for the Alamouti scheme presented in Chapter 4. Hence for this particular setup the cardinality of effectively different subsets is given by the number of combinations of n_t out of N_t elements without observing order:

$$q_{\text{eff}} = \frac{N_t!}{n_t!(N_t - n_t)!} = \binom{N_t}{n_t} \tag{2.30}$$

or specifically for $n_t = 2$ (since the Alamouti scheme uses two transmit antennas):

$$q_{\text{eff,A}} = \frac{N_t!}{2(N_t - 2)!} = \frac{1}{2}(N_t^2 - N_t) \ . \tag{2.31}$$

Furthermore, when considering the extended Alamouti scheme analyzed in Chapter 5 it is shown that swapping the order of distinct antenna-pairs inside a chosen subset produces a *different* result. Thus the number of effectively different subsets is larger than q_{eff} given by (2.30) but smaller than q in (2.29). The exact number will be presented in Chapter 5.

The remaining question is how to encode this integer number that designates the subset index in an efficient manner. To address this problem two aspects have to be considered:

1. Information content of the optimum subset index number
2. Bit-space allocation in the uplink packets carrying the feedback information

In this thesis the following assumed: The occurrence of all effectively different subsets is equally probable. It is easily verified that this is exact as long as the random variables entering the function of the selection criterion are statistically independent (i.e for uncorrelated channels). However, when the coefficients of the channel become statistically dependent this behavior is not guaranteed anymore. It was observed in the simulations that in a heavily correlated environment the number of frequently chosen subsets rapidly drops to a relatively small value.

This offers the possibility of devising a system that adapts the number of currently transmitted feedback bits to the long term channel correlation properties. A dynamic bit allocation in the uplink packets would then result in a lower average feedback bit transmission length. However, that specific subject is not examined further in this work.

Sticking to the above defined assumption of equal subset probability the following is assumed:

Each subset i occurs with probability:

$$p_i = \frac{1}{q_{\text{eff}}} \quad , \quad 1 \leq i \leq q_{\text{eff}}$$

and the mean information content (in bits) is expressed by the binary entropy [23] resulting in:

$$b_{\text{feedback}} = \sum_{i}^{q_{\text{eff}}} p_i \log_2(\frac{1}{p_i}) = \log_2(q_{\text{eff}}) \; . \tag{2.32}$$

Uplink packets carrying this feedback information usually contain additional signalling and forward error correction (FEC) information. Thus, joint coding of the whole packet contents maybe even allows a subset index with cardinality not equal to a power of two to be transported efficiently. Thus b_{feedback} is defined to be the feedback bit length without rounding it up to the nearest integer.

Chapter 3

Antenna Selection Systems

This chapter analyzes the behavior of a simple communication scheme that applies no space-time coding at all, thus only one antenna is used for transmission. The respective receive selection system processes the signal from only one out of N_r available receive antennas whereas the transmit selection case is realized by letting the transmitter use one out of the total N_t available transmit antennas.

The analysis procedure in the succeeding chapters is similar to the structure of this introductional preface where the following schedule is adopted:

1. Detailed description of the specific transmission system.
2. Analysis of the non-selective case and presentation of an analytic expression for the instantaneous BER (for a given channel realization).
3. Application of the antenna selection and formulation of possible selection criteria.
4. Analysis of average BER for receive and transmit selection systems as a function of $\frac{E_b}{N_0}$ by presenting simulation results.
5. Evaluating the gains in diversity and average $\frac{E_b}{N_0}$ achieved by the respective selection methods.

3.1 Transmission Scheme

In this simple case the actual communication only involves a single antenna on both sides. For this reason the complex channel gain from the trans-

mit antenna to the receive antenna is simply denoted by h in the following equations.

The received signal during a given symbol cycle is trivially obtained as:

$$y = hs + n$$

and after matched filtering (multiplication with the complex conjugate of h) given by:

$$z = |h|^2 s + h^* n \ .$$

Subsequent normalization yields the input for the symbol slicer

$$\tilde{s} = \frac{1}{|h|^2} z = s + \frac{n}{h} \ . \tag{3.1}$$

Since the noise phase is uniformly distributed and statistically independent of the channel phase (3.1) can be rewritten as:

$$\tilde{s} = s + \tilde{n} \tag{3.2}$$

with the scaled noise samples

$$\tilde{n} = \frac{n}{|h|} \ .$$

Thus for the considered system the error probability of a single transmitted QPSK symbol s corrupted by additive white gaussian noise with variance:

$$\sigma_{\tilde{n}}^2 = \frac{\sigma_n^2}{|h|^2} = \frac{N_0}{|h|^2} \tag{3.3}$$

needs to be evaluated.

Error Probability

Noise statistics are invariant to rotation in the complex plane, the constellation is quadratically symmetric and the symbols are equally probable. These assumptions made in Chapter 2 allow to calculate the bit error probability easily.

For the applied QPSK symbol constellation the following two mutually exclusive symbol error events need to be distinguished:

- Nearest neighbor symbol error $\mathcal{E}_1$.
- Diagonal symbol error $\mathcal{E}_2$.

Let d be the euclidian distance between two nearest neighbor symbol constellation points and $\sigma_{\tilde{n}}^2$ the variance of the scaled complex noise from (3.2).

The respective probabilities for $\mathcal{E}_1$ and $\mathcal{E}_2$ then result in:

$$P_{\mathcal{E}_1} = 2\mathcal{Q}\left(\frac{d}{\sqrt{2}\sigma_{\tilde{n}}}\right)\left[1-\mathcal{Q}\left(\frac{d}{\sqrt{2}\sigma_{\tilde{n}}}\right)\right] , \tag{3.4}$$

$$P_{\mathcal{E}_2} = \mathcal{Q}^2\left(\frac{d}{\sqrt{2}\sigma_{\tilde{n}}}\right) , \tag{3.5}$$

using the $\mathcal{Q}$-function:

$$\mathcal{Q}(\alpha) = \frac{1}{\sqrt{2\pi}}\int_{\alpha}^{\infty} e^{-\frac{1}{2}\zeta^2} d\zeta \quad , \quad \alpha \in \mathbb{R}$$

which is strictly decreasing for increasing arguments. For the non-space-time coded system considered here the emitted energy per bit per symbol cycle is related to d via:

$$d = 2\sqrt{E_b} .$$

Consequently, the argument in (3.4) and (3.5) works out to:

$$\frac{d}{\sqrt{2}\sigma_{\tilde{n}}} = \sqrt{2|h|^2\frac{E_b}{N_0}} .$$

Now only one out of the two bits transported by the symbol is distorted when $\mathcal{E}_1$ occurs, whereas in case of $\mathcal{E}_2$ both bits are erroneous. Thus the total bit error probability amounts to:

$$P_b = \frac{1}{2}(P_{\mathcal{E}_1} + 2P_{\mathcal{E}_2}) = \frac{1}{2}P_{\mathcal{E}_1} + P_{\mathcal{E}_2} = \mathcal{Q}\left(\sqrt{2|h|^2\frac{E_b}{N_0}}\right) .$$

In this thesis the complementary error function defined by:

$$\begin{aligned} \mathrm{erfc}(\alpha) &= \frac{2}{\sqrt{\pi}}\int_{\alpha}^{\infty} e^{-\zeta^2} d\zeta \quad , \quad \alpha \in \mathbb{R} , \\ \mathrm{erfc}(\alpha) &= 2\mathcal{Q}\left(\sqrt{2}\alpha\right) , \end{aligned}$$

is utilized to present analytic bit error rate expressions mainly because it is also preferred in most of the cited publications and directly available as a function call in MATLAB.

The exact expression of the bit error rate for a given channel realization then finally yields:

$$\mathrm{BER}_{|h|^2} = \frac{1}{2}\mathrm{erfc}\left(\sqrt{|h|^2\frac{E_b}{N_0}}\right) . \tag{3.6}$$

3.2 Optimum Selection Criterion

The optimum selection rule is obvious: Maximum absolute value of channel path gain from chosen transmit antenna to chosen receive antenna. The complexity is very low since it only requires a single search operation over all available channel coefficients.

Receive Selection

This system is equipped with N_r receive antennas and the selection logic simply needs to determine one element out of the estimated SIMO channel vector $\mathbf{h} = [h_1\, h_2\, \ldots\, h_{N_r}]^T$ via:

$$i = \underset{1 \le i \le N_r}{\arg\max}\ |h_i| \ . \tag{3.7}$$

Transmit Selection

Here, one out of the available transmit antennas is selected by computing:

$$j = \underset{1 \le j \le N_t}{\arg\max}\ |h_j| \ . \tag{3.8}$$

Obviously, the performance of the receive selection system is identical to the transmit selection system if $N_r = N_t$. The differences become manifest in the system structure only.

In the transmit selection case a feedback link is required, the number of effectively different subsets is simply given by N_t and respective feedback bit length yields:

$$b_{\text{feedback}} = \log_2(N_t) \ .$$

Combined Selection

The combined selection algorithm is mathematically represented as:

$$i, j = \underset{1 \le i \le N_r\ ,\ 1 \le j \le N_t}{\arg\max}\ |h_{i,j}| \tag{3.9}$$

which selects one element of the estimated MIMO channel matrix (2.4):

$$\mathbf{H} = \begin{bmatrix} h_{11} & h_{12} & \ldots & h_{1N_t} \\ h_{21} & h_{22} & \ldots & h_{2N_t} \\ \vdots & \vdots & \ddots & \vdots \\ h_{N_r1} & h_{N_r2} & \ldots & h_{N_rN_t} \end{bmatrix} \ .$$

Again the feedback bit length is given by the dual logarithm of the number of available transmit antennas.

Equations (3.7) - (3.9) hint at some major drawback of any channel-adaptive antenna selection scheme: It lowers hardware requirements during the actual transmission but it requires the estimation of all channel coefficients (in this case at least their amplitudes) in the first place. Obviously, a large number of available antennas makes it difficult to complete this task within narrow time constraints.

Prior to the presentation of numerical simulation figures for the antenna selection systems the (analytic) results for a set of non-selective setups are evaluated. By doing so the potential of selective systems is then easily assessed by comparing them to their full complexity counterparts or systems with no multiple antennas to select from at all.

3.3 Reference Systems

Non-selective single antenna system

As a starting point the result for the system discussed in Section 3.1 without any applied selection is evaluated. In order to obtain an expression for the average BER the instantaneous result from (3.6) needs to be averaged over the realizations of $|h|^2$. Referring to Section 2.2 this is done by using the central chi-squared distribution (2.10) and results in the following double integral:

$$\begin{aligned} \overline{\mathrm{BER}} &= \int_0^\infty \mathrm{BER}_{|h|^2} pdf_{|h|^2}(\xi) d\xi = \\ &\frac{1}{\sqrt{\pi}} \int_0^\infty e^{-\xi} \int_{\sqrt{\xi \frac{E_b}{N_0}}}^\infty e^{-\zeta^2} d\zeta d\xi \ . \end{aligned} \tag{3.10}$$

The analytical result is given by [19]:

$$\overline{\mathrm{BER}} = \frac{1}{2} \left(1 - \sqrt{\frac{\frac{E_b}{N_0}}{1 + \frac{E_b}{N_0}}} \right) \ . \tag{3.11}$$

In Figure 3.1 the plot of (3.11) is shown and also compared to the results of an appropriate Monte-Carlo simulation. The scaling of the ordinate is intentionally not adapted to the results in order to be consistent with the subsequent figures.

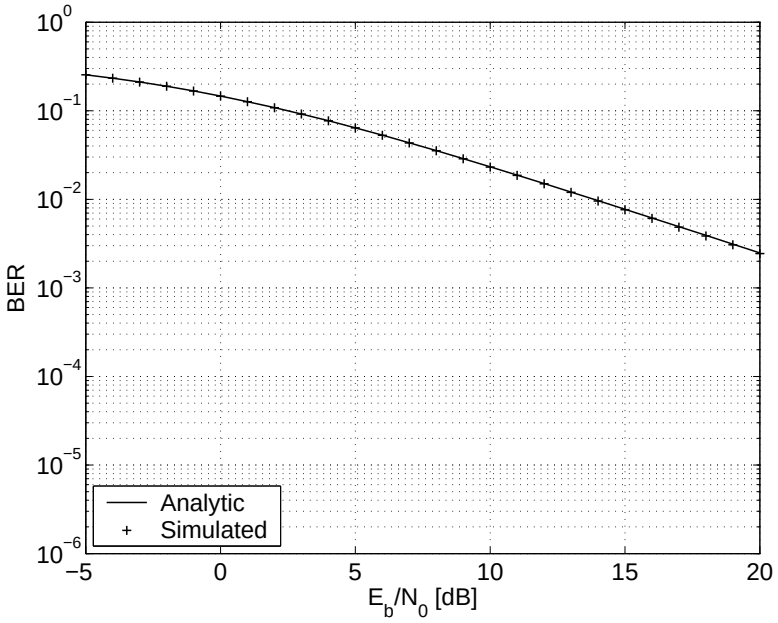

Figure 3.1: Non-space-time coded system without antenna selection.

Ideal Receive Diversity System

The next reference system utilizes all of the available N_r receive antennas simultaneously. With $\mathbf{h} = [h_1\, h_2\, \ldots\, h_{N_r}]^T$ being the appropriate SIMO channel vector the transmission is characterized by:

$$\mathbf{y} = \mathbf{h}s + \mathbf{n}\ .$$

Here $\mathbf{y} = [y_1\, y_2\, \ldots\, y_{N_r}]^T$ accumulates the received signals from the different antennas by stacking them in a column vector and the respective noise samples are identically given by $\mathbf{n} = [n_1\, n_2\, \ldots\, n_{N_r}]^T$. Maximum-ratio-receive-combining (MRRC) is done by:

$$z = \mathbf{h^H y} = \mathbf{h^H}\,\mathbf{h}\,s + \mathbf{h^H n}$$

and subsequent normalization yields:

$$\tilde{s} = s + \frac{h_1^* n_1 + h_2^* n_2 + \cdots + h_{N_r}^* n_{N_r}}{|h_1|^2 + |h_2|^2 + \cdots + |h_{N_r}|^2} = s + \tilde{n}\ . \tag{3.12}$$

According to (2.27) the noise components from different receive antennas are statistically independent, thus the variance of the total noise $\tilde{n}$ is obtained

by simply adding the variances of the individual components in (3.12) which results in:

$$\sigma_{\tilde{n}}^2 = \frac{N_0}{|h_1|^2 + \cdots + |h_{N_r}|^2} = \frac{N_0}{\|\mathbf{h}\|_F^2} \tag{3.13}$$

with $\|\mathbf{h}\|_F$ being the Frobenius norm of the estimated SIMO channel vector $\mathbf{h} = [h_1\, h_2\, \ldots\, h_{N_r}]^T$. For an arbitrary complex matrix $\mathbf{A}$ with elements a_{ij} the Frobenius norm is defined as:

$$\|\mathbf{A}\|_F = \sqrt{\sum_{i=1}^{m}\sum_{j=1}^{n} |a_{ij}|^2}\ .$$

Since (3.13) is an equivalent to (3.3) the instant bit error ratio is obtained as:

$$\mathrm{BER}_{\|\mathbf{h}\|_F^2} = \frac{1}{2}\mathrm{erfc}\left(\sqrt{\|\mathbf{h}\|_F^2 \frac{E_b}{N_0}}\right)\ . \tag{3.14}$$

In order to determine the corresponding average bit error ratio the distribution of $\|\mathbf{h}\|_F^2$ needs to be evaluated which requires the definition of the chi-squared distribution in Section 2.2 to be extended to more than two degrees of freedom.

A random variable Y is known to be central chi-squared distributed with n degrees of freedom if it is composed of n i.i.d. zero mean real valued gaussian elements X_i via:

$$Y = \sum_{i=1}^{n} X_i^2\ .$$

The pdf of Y is then given by [19]:

$$pdf_Y(\alpha) = \frac{1}{\sigma_X^n 2^{n/2}\Gamma(\frac{1}{2}n)}\alpha^{n/2-1}e^{-\alpha/2\sigma_X^2}\ , \quad 0 \le \alpha\ , \tag{3.15}$$

with σ_X^2 being the variance of the original random variables X_i. Here, Γ denotes the gamma function:

$$\begin{aligned}\Gamma(\beta) &= \int_0^\infty t^{\beta-1}e^{-t}dt\ , \quad 0 < \beta\ ,\\ \Gamma(\beta) &= (\beta-1)!\ , \quad \beta \in \mathbb{N}\ .\end{aligned}$$

Obviously, for the uncorrelated channel case $\|\mathbf{h}\|_F^2$ is comprised of a sum of squared variables whose real and imaginary parts are i.i.d zero mean real

valued gaussian distributed with variance $\sigma^2 = 0.5$ (c.f. Section 2.2).

Thus the pdf of $\|\mathbf{h}\|_F^2$ for the considered SIMO case is given by the central-chi-squared distribution (3.15) with $n = 2N_r$ and $\sigma_X^2 = 0.5$:

$$pdf_{\|\mathbf{h}\|_F^2}(\alpha) = \frac{1}{(N_r - 1)!}\alpha^{N_r - 1}e^{-\alpha} , \quad 0 \leq \alpha .$$

Now the average BER is calculated completely analogous to (3.10):

$$\overline{\mathrm{BER}} = \int_0^\infty \mathrm{BER}_{\|\mathbf{h}\|_F^2} pdf_{\|\mathbf{h}\|_F^2}(\xi) d\xi .$$

Again [19] provides an analytic result:

$$\overline{\mathrm{BER}} = \left(\frac{1-\mu}{2}\right)^{N_r} \sum_{l=0}^{N_r - 1} \binom{N_r - 1 + l}{l} \left(\frac{1+\mu}{2}\right)^l , \tag{3.16}$$

with

$$\mu = \sqrt{\frac{\frac{E_b}{N_0}}{1 + \frac{E_b}{N_0}}} .$$

Figure 3.2 presents the results of (3.16) for $N_r = 1 \ldots 8$.

At this point the term **diversity order** is introduced. It corresponds to the number of *independent* channel paths that are available to combine the received signal. Hence for the currently considered ideal receive diversity systems the attainable diversity order D is equal to the number of receive antennas:

$$D = N_r$$

Ideal Transmit Diversity System

A MISO system with N_t *simultaneously* active transmit antennas and one receive antenna is analyzed similar to the SIMO system considered above. The required orthogonal space-time block codes for an arbitrary number of transmit antennas do exist as has been shown in [10], but in the introduction of Chapter 5 some important remarks on STBCs for more than two transmit antennas will point out that the maximum data rate of these codes is not equal to the as yet considered non-space-time coded transmission or the Alamouti STBC which will be presented in the next chapter. One should

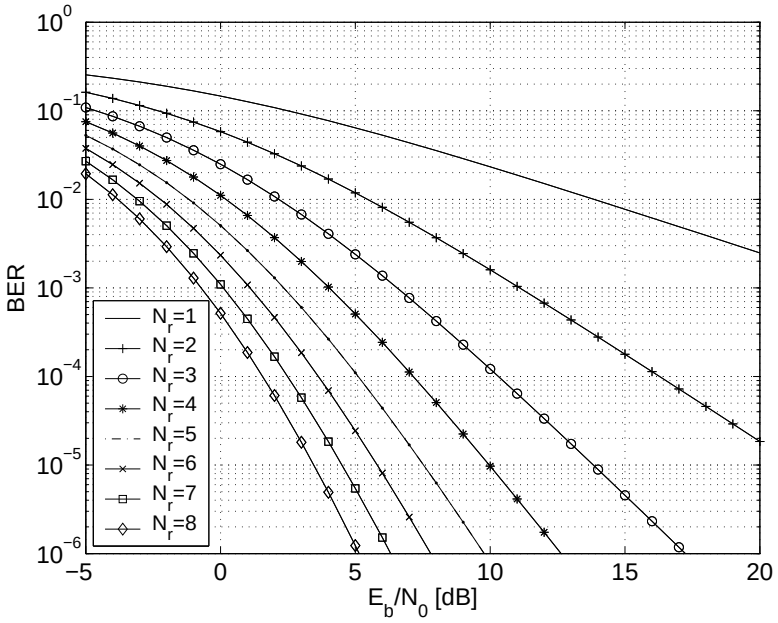

Figure 3.2: Full complexity ideal receive diversity systems, $N_t = 1, n_r = N_r$.

keep that in mind when comparing transmit antenna selection systems with these ideal transmit diversity systems.

Using orthogonal space-time coding (c.f. Chapter 5 and [10]) the instant BER works out to:

$$\mathrm{BER}_{\|\mathbf{h}\|_F^2} = \frac{1}{2}\mathrm{erfc}\left(\sqrt{\frac{\|\mathbf{h}\|_F^2}{N_t}\frac{E_b}{N_0}}\right) \tag{3.17}$$

with $\|\mathbf{h}\|_F^2$ now being the Frobenius norm of the corresponding MISO channel vector $\mathbf{h} = [h_1\, h_2\, \ldots\, h_{N_t}]$. Equation (3.16) again provides the average BER with a slightly altered of definition of μ:

$$\mu = \sqrt{\frac{\frac{E_b}{N_0}}{N_t + \frac{E_b}{N_0}}}$$

and the resulting curves are presented in Figure 3.3.

Obviously, every single plot for a given N_t presented in Figure 3.3 can be made congruent to the corresponding curve for $N_r = N_t$ in Figure 3.2 when shifted to the left by $1.5\,N_t\,[\mathrm{dB}]$. This change in average SNR is a

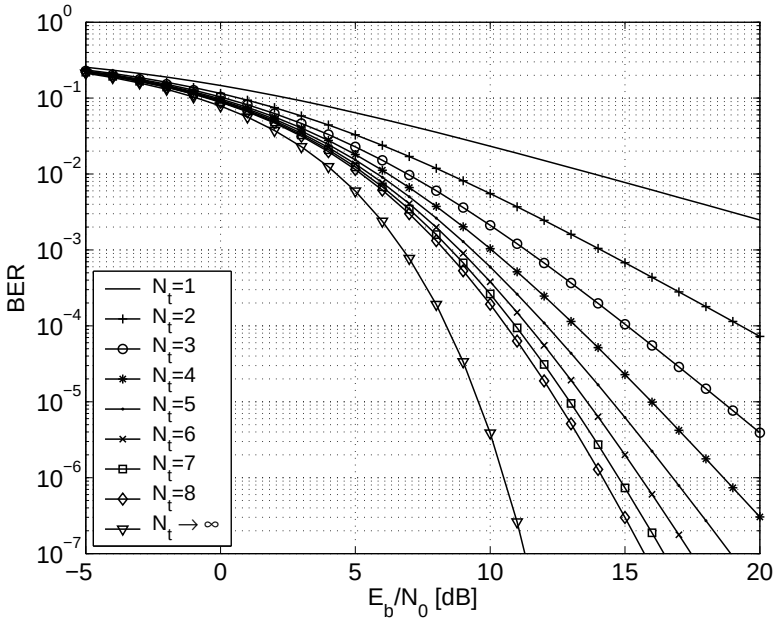

Figure 3.3: Full complexity ideal transmit diversity systems, $n_t = N_t, N_r = 1$.

consequence of subdividing the total transmit power onto N_t antennas in the case of transmit diversity.

The number of independent channel paths used to obtain the received signal is analogously given by the number of transmit antennas. Consequently, the attainable diversity order yields:

$$D = N_t \ .$$

Additionally, Figure 3.3 is complemented by the result for $N_t \to \infty$. Evaluating the limit:

$$\lim_{N_t \to \infty} \frac{|h_1|^2 + |h_2|^2 + \cdots + |h_{N_t}|^2}{N_t} = 1$$

shows that the case of $N_t \to \infty$ is equal to the transmission over a fixed channel with $|h|^2 = 1$:

$$\overline{\mathrm{BER}} = \frac{1}{2}\mathrm{erfc}\left(\sqrt{\frac{E_b}{N_0}}\right)$$

3.3.1 Diversity Estimation

The remaining question is how to estimate the diversity order offered by the investigated selective systems. As an example, the receive selection system

will be clearly inferior to the full complexity ideal receive diversity system even when the number of available antennas N_r is equal. A method that allows the accurate quantification of differences in diversity and average SNR is needed. In the following three possible ways of diversity estimation are presented.

- Matching the average bit error ratio curve with an appropriate ideal diversity result by performing a parallel shift in the graph.
- Measuring the slope of the curve.
- Evaluating the statistical properties of the argument in the instantaneous BER expression and matching it to an equivalent chi-squared distribution.

The first method is intuitive. If there exists an ideal receive (or transmit) diversity system that exhibits the exact same progression of $\overline{\mathrm{BER}}$ with a constant difference of $\frac{E_b}{N_0}$ [dB] in the double logarithmic plot (i.e the curves are parallel) one can conclude that the diversity orders offered by both compared systems are equal.

The second method is based on the assumption that $\overline{\mathrm{BER}}$ for $\frac{E_b}{N_0} \to \infty$ is given by [6]:

$$\lim_{\frac{E_b}{N_0}\to\infty} \overline{\mathrm{BER}} = C \left(\frac{E_b}{N_0}\right)^{-D} ,$$

with C being a real valued positive constant that generally also depends on D but is independent of $\frac{E_b}{N_0}$. Evaluating the slope of the bit error ratio graph in the high SNR region via:

$$D = -\lim_{\frac{E_b}{N_0}\to\infty} \frac{\mathrm{d}\log(\overline{\mathrm{BER}})}{\mathrm{d}\log(\frac{E_b}{N_0})}$$

thus offers an alternative way to rate the offered diversity order from a numerical simulation figure. It is clear that this approach systematically underestimates D since $\overline{\mathrm{BER}}$ is a strictly decreasing function for the systems considered here, and the asymptotic slope cannot be observed from numerical results.

The third method utilizes means of statistical comparison: Let the instant BER for any given antenna selection system be a closed analytic expression in the form of:

$$\mathrm{BER}_\alpha = \frac{1}{2}\mathrm{erfc}\left(\sqrt{\alpha\frac{E_b}{N_0}}\right) , \quad 0 \le \alpha .$$

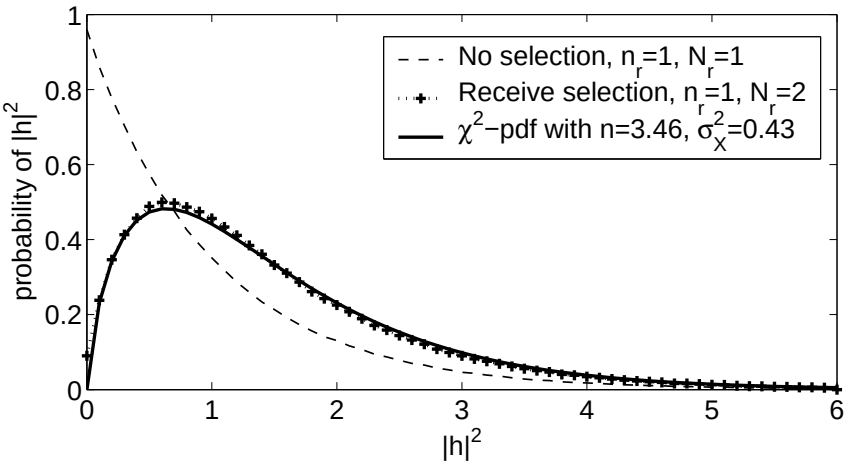

Figure 3.4: Test

Generally, the distribution of α completely defines the resulting system performance and is determined by the original distribution of channel coefficients and the applied selection algorithm.

If it is possible to find a chi-squared probability density function (also allowing for non-integer degrees of freedom) that *exactly* matches the pdf of α one could accurately quantify the respective diversity order by:

$$D = \frac{1}{2}n \ .$$

Furthermore, if the variance σ_X^2 of the matched chi-squared distribution is unequal to $\sigma^2 = 0.5$, the deviation would precisely define a change in average SNR.

In Figure 3.4 the histograms of $|h|^2$ for the non-space-time coded non-selective system as well as for the corresponding receive selection system with two available receive antennas are displayed (based on 10^6 randomly generated channel realizations). By doing an exhaustive search over all possible values of n and σ_X^2 (with a stepsize of 0.01) the best fitting[1] chi-squared distribution with $n = 3.46$ was found.

However, the resulting estimated diversity order of $D = 1.73$ is 13 percent lower than $D = 2$ which is obtained by applying the first mentioned method of diversity estimation. Comparing the receive selection system with the ideal receive diversity system with $n_r = N_r = 2$ (c.f Section 3.4) shows that the curves are exactly alike when the latter is shifted to the right by 1.5 dB.

[1] In this context "best fitting" means minimum sum of squared error between the histogram points and the respective chi-squared pdf function.

It is therefore concluded that the distribution of $|h|^2$ for selective cases cannot be matched to a chi-squared distribution with reasonable precision.

As a consequence, the first two methods of diversity estimation are favored in this thesis since they reliably deliver more accurate results.

3.4 Simulation Results

In the following the numerical simulation figures for the considered antenna selection systems are presented. The results for uncorrelated channels are grouped in receive selection and transmit selection cases. The analysis of receive selection in the presence of spatial channel correlation at the receiver side is exemplarily depicted by the last two figures.

3.4.1 Uncorrelated Channels

Receive Selection

- **Figure 3.5** shows the results of the non-space-time coded receive antenna selection system for $N_r = 1 \dots 8$.
- **Figure 3.6** compares the receive selection performance for $N_r = 2, 3, 4$ with the corresponding full complexity ideal receive diversity systems for $n_r = N_r = 2, 3, 4$.

  Obviously the diversity gain $D = N_r$ for the full complexity system is maintained even when only one out of the available receive antennas is used.
- **Figure 3.7** shows the progression of the resulting SNR loss with increasing number of available receive antennas.

Transmit Selection

- **Figure 3.8** compares the results of the non-space-time coded transmit antenna selection system with the ideal transmit diversity system with $n_t = N_t = 2, 3, 4$. Obviously, they also differ only in a change of average SNR but here the selection systems perform *better*. This gain can be interpreted as a **closed loop selection gain** and is due to the fact that the transmit selection system only uses the best antenna to emit all of the available transmit power whereas the ideal transmit diversity system equally distributes the power over all antennas (even those with very high path attenuation to the receiver).

- **Figure 3.9** plots the closed loop selection gain over the number of available transmit antennas.
- **Figure 3.10** displays the closed loop selection gain over the number of required feedback bits. Obviously, there exists a close relation between the amount of available feedback information and the achievable gain over the non-selective full complexity system.

Combined Selection

It is easily concluded that the combined selection performance for N_t and N_r available antennas at the transmitter and the receiver respectively is equal to exclusive receive selection if the number of available receive antennas equals $N_t\,N_r$. So the result for $N_r = 8$ in Figure also represents combined selection with $N_t = 4, N_r = 2$ or $N_t = 2, N_r = 4$ etc.

3.4.2 Correlated Channels

- **Figure 3.11** showcases the degradation of receive selection performance when the correlation at the receiver is increased from $\rho_r = 0$ to $\rho_r = 0.5$, 0.75, 0.95, 1 for the case of $N_r = 4$.
- **Figure 3.12** finally further demonstrates the relation between diversity and channel correlation by plotting the achievable diversity order over the number of available receive antennas with ρ_r as a parameter.

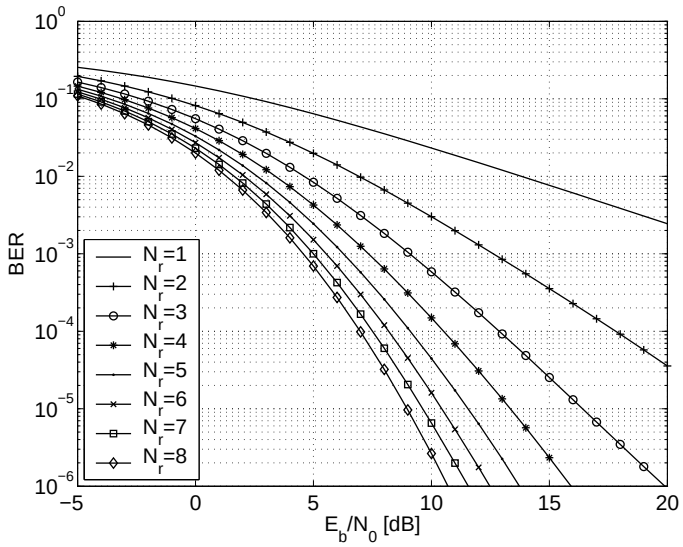

Figure 3.5: Receive selection performance, $N_r = 1 \ldots 8$.

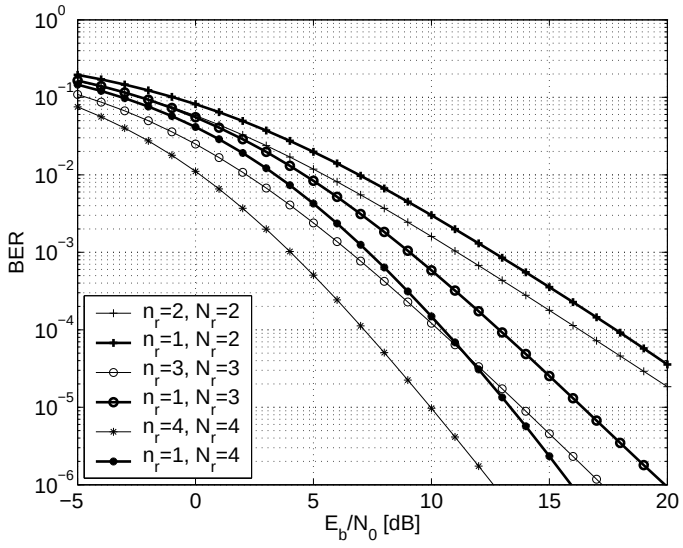

Figure 3.6: Receive selection compared to the respective full complexity systems ($n_r = N_r$) for $N_r = 2, 3, 4$.

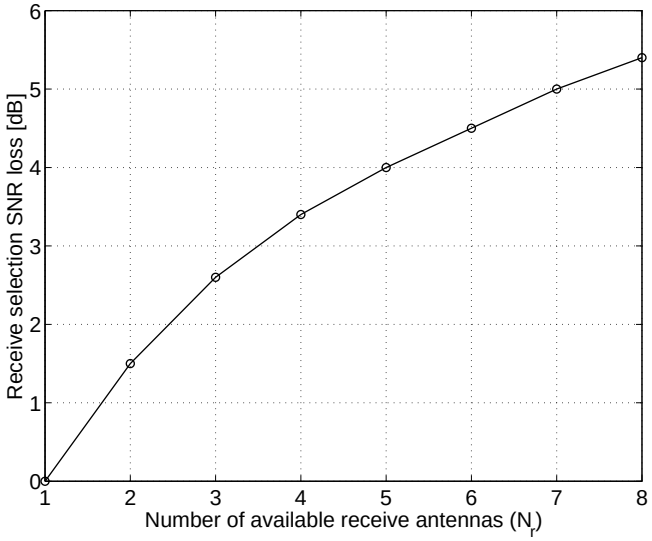

Figure 3.7: Receive selection SNR loss to the respective full complexity system, $N_r = 1 \ldots 8$.

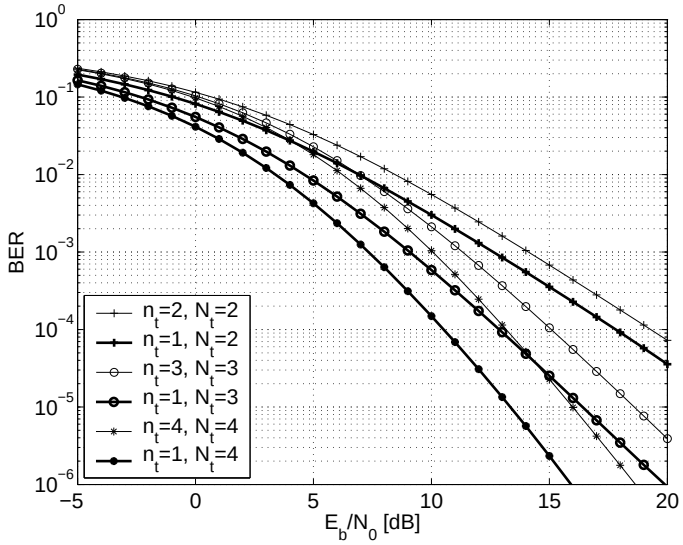

Figure 3.8: Transmit selection with $N_t = 2, 3, 4$ available antennas at the transmitter, compared with the corresponding full complexity systems ($n_t = N_t$).

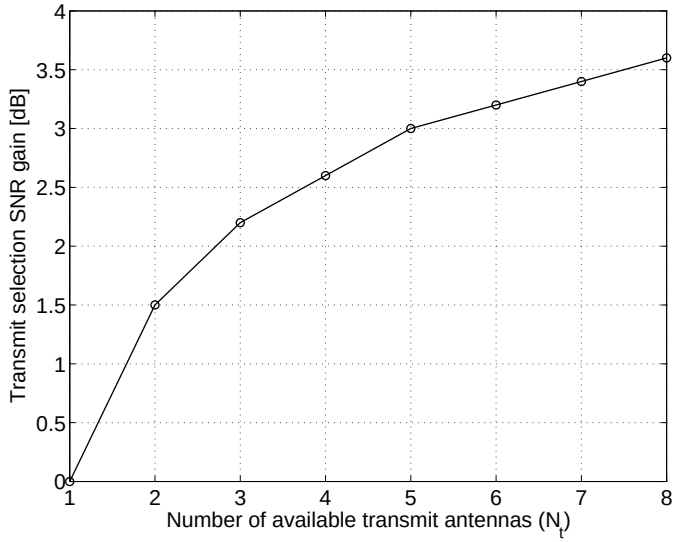

Figure 3.9: Transmit selection gain for $N_t = 1 \ldots 8$.

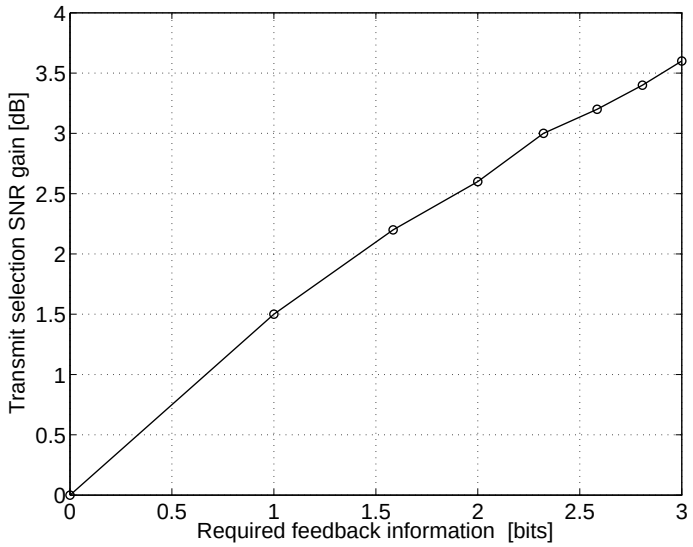

Figure 3.10: Relation between transmit selection gain and available feedback information

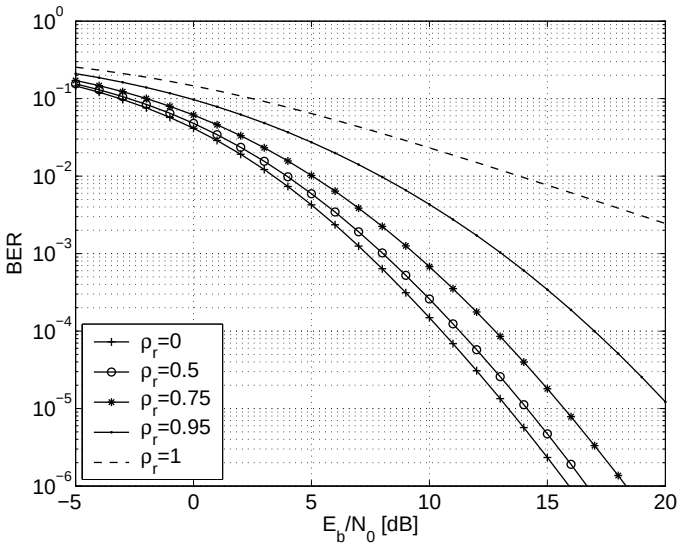

Figure 3.11: Degradation of receive selection performance in the presence of receive correlation ρ_r.

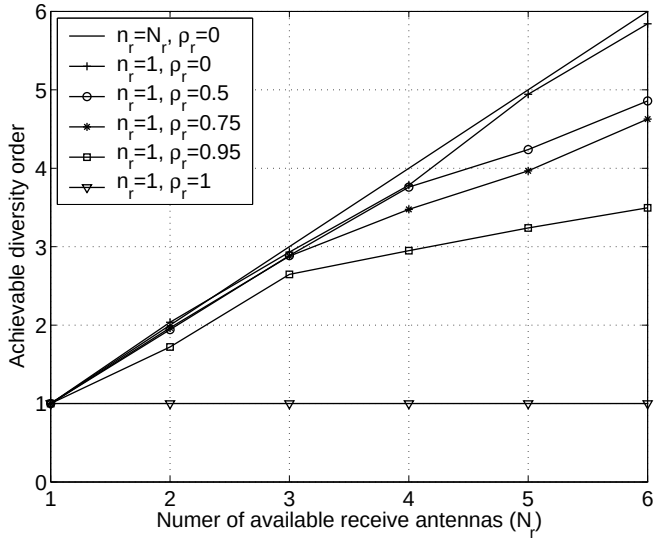

Figure 3.12: Achievable diversity order in the case of receive selection over the number of available antennas, parameterized by ρ_r.

Chapter 4

Alamouti STBC

In the following antenna selection is applied to a system that utilizes the well known Alamouti transmit diversity scheme. This STBC was proposed in [24] and uses two transmit antennas and one receive antenna simultaneously. Its most attractive features are given by:

- Diversity order of two.
- Only one receive antenna.
- Low complexity detection principle.
- No feedback requirements.

A diversity order of two is also obtainable by the ideal receive diversity system (with $N_r = 2$) that has been presented as a reference in the previous chapter. However, the Alamouti scheme allows to shift the multiplicity of RF-chains from the receiver to the transmitter, making it an attractive method for enhancing the downlink to small mobile units with a low power consumption profile. The detection algorithm complexity is low for both schemes, optimum maximum-likelihood detection performance is attainable with simple linear processing.

To sum up, the Alamouti STBC transmission is capable of delivering the same diversity order as the MRRC system while utilizing only one receive antenna. The performances of the two schemes only differ by a constant penalty of 3dB in average SNR for the Alamouti scheme. The reason for this is simply because the total transmit power is being split up on the two transmit antennas.

At this point some general remarks on the application of space-time coding are indicated. Again comparing it with some receive diversity technique

	antenna 1	antenna 2
first symbol cycle	s_1	s_2
second symbol cycle	s_2^*	$-s_1^*$

Table 4.1: The Alamouti encoding procedure

like MRRC two major differences arise. The first issue is the unavoidable decoding delay that is inherent to the space-time coding principle.

Secondly, channel estimation issues are more complex to solve since the paths from multiple transmit antennas need to be estimated, thus either alternate pilot insertion or orthogonal pilot signals need to be employed.

However, these drawbacks are moderate considering the Alamouti scheme that is analyzed in the following, since it only introduces the minimal decoding delay of one additional symbol period and utilizes only two transmit antennas.

4.1 The Alamouti Transmission Scheme

The to-be transmitted bitsequence is mapped to symbols and the resulting symbol stream is subsequently grouped into blocks being two symbols long. These blocks are then successively transmitted via two transmit antennas during two symbol intervals in the following fashion.

Let s_1 and s_2 be the elements of one of the above mentioned symbol blocks. According to Table 4.1 an Alamouti STBC scheme is realized by transmitting s_1 via the first antenna and s_2 via the second antenna during the first symbol period. Whilst the next symbol cycle s_2^* is emitted from antenna one and $-s_1^*$ from antenna two respectively.

It is assumed that the channel path gains from the two transmit antennas to the single receive antenna (denoted by h_1 and h_2) are not changing during those two symbol cycles.

The receive signals r_1 and r_2 for the two considered time intervals are then obtained as:

$$\begin{aligned} r_1 &= h_1 s_1 + h_2 s_2 + n_1 \\ r_2 &= h_1 s_2^* - h_2 s_1^* + n_2 \end{aligned} \tag{4.1}$$

with n_1 and n_2 being the noise samples during cycle one and two respectively. See Figure 4.1 for a graphical representation of (4.1). At the receiver the

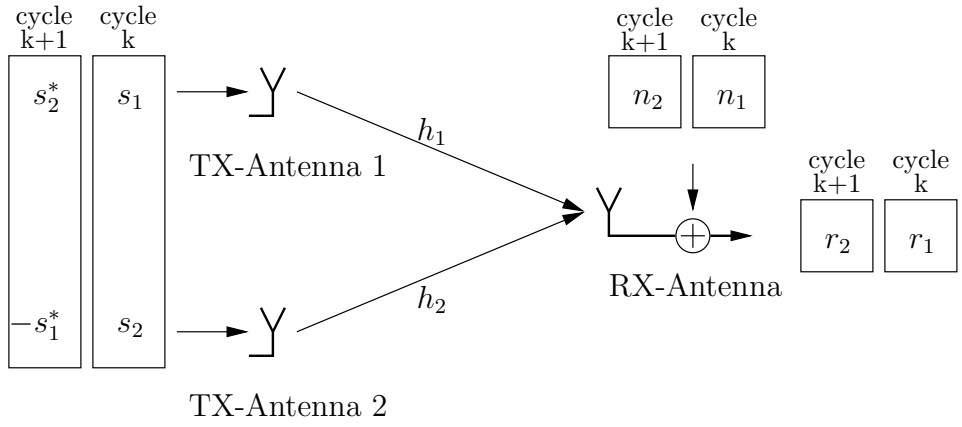

Figure 4.1: The Alamouti transmission procedure

following combining scheme is applied:

$$\begin{aligned} z_1 &= h_1^* r_1 - h_2 r_2^* = (|h_1|^2 + |h_2|^2) s_1 + h_1^* n_1 - h_2 n_2^* \\ z_2 &= h_2^* r_1 + h_1 r_2^* = (|h_1|^2 + |h_2|^2) s_2 + h_1 n_2^* + h_2^* n_1 \end{aligned} \tag{4.2}$$

and after subsequent normalization an equivalent to (3.12) is obtained:

$$\tilde{s}_1 = s_1 + \tilde{n}_1 \quad , \quad \tilde{n}_1 = \frac{h_1^* n_1 - h_2 n_2^*}{|h_1|^2 + |h_2|^2} \tag{4.3}$$

$$\tilde{s}_2 = s_2 + \tilde{n}_2 \quad , \quad \tilde{n}_2 = \frac{h_1 n_2^* + h_2^* n_1}{|h_1|^2 + |h_2|^2} \; . \tag{4.4}$$

Analog to (3.13) the variances of $\tilde{n}_1$ and $\tilde{n}_2$ work out to:

$$\sigma_{\tilde{n}_1}^2 = \sigma_{\tilde{n}_2}^2 = \frac{\sigma_n^2}{|h_1|^2 + |h_2|^2} = \frac{N_0}{\|\mathbf{h}\|_F^2} \; . \tag{4.5}$$

More importantly, the two noise samples $\tilde{n}_1$ and $\tilde{n}_2$ are uncorrelated since:

$$\mathrm{E}\left\{\tilde{n}_1 \tilde{n}_2^*\right\} = \mathrm{E}\left\{\tilde{n}_1^* \tilde{n}_2\right\} = 0 \; . \tag{4.6}$$

This property allows to conclude that optimum performance in the maximum-likelihood sense is accomplished by *seperate* detection of the respective final symbol estimates based on $\tilde{s}_1$ and $\tilde{s}_2$ using the symbol slicer.

Observing (4.5) and (4.6) it becomes obvious that the instantaneous BER for the Alamouti STBC is almost identical to the result for a ($M_r = 2$) MMRC receive diversity system (3.14). One only needs to keep in mind that

the transmit symbols s_1 and s_2 in (4.3) and (4.4) are scaled by $\frac{1}{\sqrt{2}}$ (due to the transmit power constraint). The final result yields:

$$\mathrm{BER}_{\|\mathbf{h}\|_F^2} = \frac{1}{2}\mathrm{erfc}\left(\sqrt{\frac{\|\mathbf{h}\|_F^2}{2N_0}}\right) \tag{4.7}$$

and is indeed equal to the ideal transmit diversity BER in (3.17) for $M_t = 2$. Thus the diversity order of two is guaranteed.

4.1.1 STBC-Matrix Notation

For more complex space-time block codes the previous way of description becomes impractical. In the following a different mathematical representation of the Alamouti scheme is given, outlining a straightforward and more general way to describe space-time block codes.

Starting point is the formulation of the space-time code matrix $\mathbf{S}$:

$$\mathbf{S} = \begin{bmatrix} s_1 & s_2 \\ s_2^* & -s_1^* \end{bmatrix} . \tag{4.8}$$

This is the matrix-equivalent to Table 4.1, thus the rows correspond to the symbol intervals and the columns identify the respective transmit antenna.

The received signals, channel path gains and noise samples are stacked in 2×1 column vectors:

$$\mathbf{r} = \begin{bmatrix} r_1 \\ r_2 \end{bmatrix}, \quad \mathbf{h} = \begin{bmatrix} h_1 \\ h_2 \end{bmatrix}, \quad \mathbf{n} = \begin{bmatrix} n_1 \\ n_2 \end{bmatrix} ,$$

and the equivalent to equation (4.1) is then given by:

$$\mathbf{r} = \mathbf{S}\mathbf{h} + \mathbf{n} . \tag{4.9}$$

Alternatively by using slightly altered noise and receive vectors:

$$\mathbf{y} = \begin{bmatrix} y_1 \\ y_2 \end{bmatrix} = \begin{bmatrix} r_1 \\ r_2^* \end{bmatrix}, \quad \mathbf{v} = \begin{bmatrix} v_1 \\ v_2 \end{bmatrix} = \begin{bmatrix} n_1 \\ n_2^* \end{bmatrix} ,$$

equation (4.9) can be rewritten as:

$$\mathbf{y} = \mathbf{H}_{\mathrm{v}}\mathbf{s} + \mathbf{v} . \tag{4.10}$$

With $\mathbf{H}_{\mathrm{v}}$ being defined by:

$$\mathbf{H}_{\mathrm{v}} = \begin{bmatrix} h_1 & h_2 \\ -h_2^* & h_1^* \end{bmatrix} .$$

Due to the similarity to the general MIMO input output-relation that has been presented in Chapter 2.3:

$$\mathbf{y} = \mathbf{H}\mathbf{s} + \mathbf{n} ,$$

$\mathbf{H}_{\mathrm{v}}$ will be termed the virtual channel matrix for the Alamouti STBC scheme. Thus, by thinking of the elements of $\mathbf{y}$ in (4.10) as originating from two receive antennas (instead of one antenna over two time slots) one could construe the (2×1) Alamouti STBC as a (2×2) spatial multiplexing transmission. The key difference lies in the inner structure of $\mathbf{H}_{\mathrm{v}}$. Unlike to a general i.i.d. MIMO channel matrix, the rows and columns of the virtual channel matrix are strictly orthogonal:

$$\mathbf{H}_{\mathrm{v}}\mathbf{H}_{\mathrm{v}}^H = \mathbf{H}_{\mathrm{v}}^H\mathbf{H}_{\mathrm{v}} = (|h_1|^2 + |h_2|^2)\mathbf{I}_2 = \|\mathbf{h}\|_F^2\mathbf{I}_2 ,$$

which establishes the significant difference to spatial multiplexing transmission where the symbols transmitted in the second timeslot are independent of the symbols in the first timeslot.

By multiplying (4.10) with the hermitian of $\mathbf{H}_{\mathrm{v}}$ the equivalent to (4.2) is obtained:

$$\mathbf{z} = \mathbf{H}_{\mathrm{v}}^H\mathbf{y} = \mathbf{H}_{\mathrm{v}}^H\mathbf{H}_{\mathrm{v}}\mathbf{s} + \mathbf{H}_{\mathrm{v}}^H\mathbf{v} .$$

And finally, since the inverse of $\mathbf{H}_{\mathrm{v}}^H\mathbf{H}_{\mathrm{v}}$ is easily obtained as:

$$[\mathbf{H}_{\mathrm{v}}^H\mathbf{H}_{\mathrm{v}}]^{-1} = \frac{1}{\|\mathbf{h}\|_F^2}\mathbf{I}_2 ,$$

the resulting equivalent to (4.5) is given by:

$$\tilde{\mathbf{s}} = [\mathbf{H}_{\mathrm{v}}^H\mathbf{H}_{\mathrm{v}}]^{-1}\mathbf{z} = \mathbf{s} + \frac{1}{\|\mathbf{h}\|_F^2}\mathbf{H}_{\mathrm{v}}^H\mathbf{v} = \mathbf{s} + \tilde{\mathbf{v}} . \tag{4.11}$$

Calculating the correlation matrix of the resulting noise vector in (4.11):

$$\mathrm{E}\left\{\tilde{\mathbf{v}}\tilde{\mathbf{v}}^H\right\} = \mathrm{E}\left\{\frac{1}{\|\mathbf{h}\|_F^2}\mathbf{H}_{\mathrm{A}}^H\mathbf{v}\left[\frac{1}{\|\mathbf{h}\|_F^2}\mathbf{H}_{\mathrm{A}}^H\mathbf{v}\right]^H\right\} = \frac{\sigma_n^2}{\|\mathbf{h}\|_F^2}\mathbf{I}_2$$

again confirms the optimality of linear detection.

4.2 Optimum Selection Criterion

Considering the analytic bit error ratio expression (4.7) the only useful selection criterion is easily formulated: maximum Frobenius norm of the selected MISO channel vector $\mathbf{h} = [h_1\, h_2]^T$.

Receive Selection

If the system is equipped with N_r receive antennas:

$$i = \underset{1 \leq i \leq N_r}{\arg\max} \left(|h_{i1}| + |h_{i2}| \right)$$

is evaluated in order to select one row out of the MIMO matrix:

$$\mathbf{H} = \begin{bmatrix} h_{11} & h_{12} \\ h_{22} & h_{22} \\ \vdots & \vdots \\ h_{N_r 1} & h_{N_r 2} \end{bmatrix} \quad \rightarrow \quad \mathbf{h}_i = \begin{bmatrix} h_{i1} & h_{i2} \end{bmatrix} .$$

Transmit Selection

Conversely, if N_t antennas are available at the transmitter:

$$i, j = \underset{1 \leq i,j \leq N_t,\, i \neq j}{\arg\max} \left(|h_i| + |h_j| \right) \tag{4.12}$$

needs to be computed in order to select two elements out of the MISO channel vector:

$$\mathbf{h} = [h_1\, h_2\, \ldots\, h_{N_t}] \quad \rightarrow \quad \mathbf{h}_{i,j} = [h_i\, h_j] .$$

Combined Selection

Combining transmit and receive selection results in a joint optimization procedure where the transmit selection algorithm outlined in (4.12) needs to be repeated for every row of the estimated MIMO matrix:

$$\mathbf{H} = \begin{bmatrix} h_{11} & h_{12} & \ldots & h_{1N_t} \\ h_{21} & h_{22} & \ldots & h_{2N_t} \\ \vdots & \vdots & \ddots & \vdots \\ h_{N_r 1} & h_{N_r 2} & \ldots & h_{N_r N_t} \end{bmatrix} = \begin{bmatrix} \mathbf{h}_1 \\ \mathbf{h}_2 \\ \vdots \\ \mathbf{h}_{N_r} \end{bmatrix} . \tag{4.13}$$

4.3 Reference Systems

In the case of Alamouti STBC transmission the system that utilizes more than one antenna for reception (i.e. the full complexity system) is yet to be specified in order to conduct a useful comparison with the receive selection setup.

In the following the standard Alamouti scheme is extended to $N_r > 1$ receive antennas while keeping the transmission procedure identical to the 2×1 case. The signals from the multiple receive antennas are maximum-ratio combined by constructing an appropriate virtual channel matrix and repeating the detection processing analogous to the single receive antenna case.

For the case of N_r receive antennas the channel is represented by the $2 \times N_r$ MIMO matrix:

$$\mathbf{H} = \begin{bmatrix} h_{11} & h_{12} \\ h_{21} & h_{22} \\ \vdots & \vdots \\ h_{N_r 1} & h_{N_r 2} \end{bmatrix} . \tag{4.14}$$

Now N_r virtual channel sub-matrices are generated by processing (4.14) row-by-row:

$$\mathbf{H}_{\mathrm{v,n}} = \begin{bmatrix} h_{n1} & h_{n2} \\ -h_{n2}^* & h_{n1}^* \end{bmatrix} \quad , \quad 1 \leq n \leq N_r$$

Stacking those 2×2 matrices on top of each other finally yields the correct virtual channel matrix for the Alamouti transmission scheme with N_r receive antennas:

$$\mathbf{H}_{\mathrm{v}} = \begin{bmatrix} h_{11} & h_{12} \\ -h_{12}^* & h_{11}^* \\ h_{21} & h_{22} \\ -h_{22}^* & h_{21}^* \\ \vdots & \vdots \\ h_{N_r 1} & h_{N_r 2} \\ -h_{N_r 2}^* & h_{N_r 1}^* \end{bmatrix} .$$

Again, the input-output relation is given by:

$$\mathbf{y} = \mathbf{H}_{\mathrm{v}} \mathbf{s} + \mathbf{v} \ ,$$

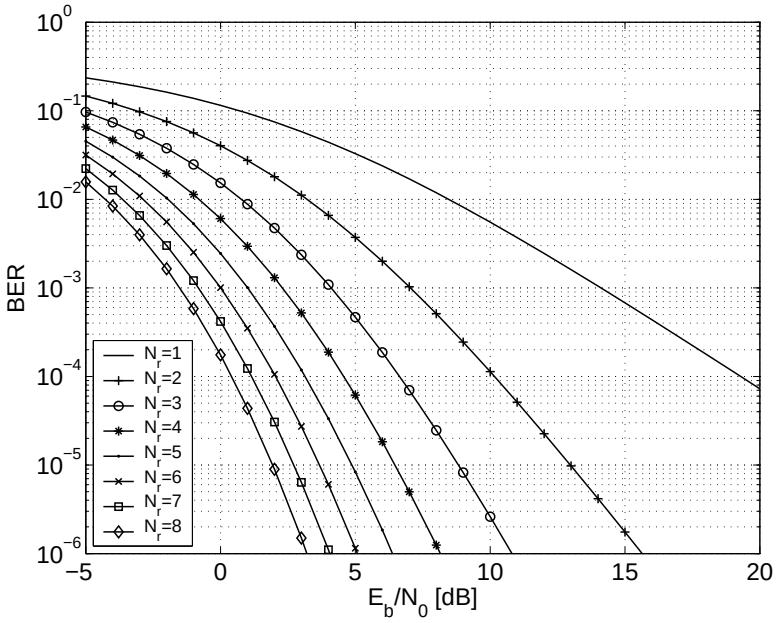

Figure 4.2: Alamouti STBC transmission system utilizing multiple receive antennas, $N_r = 1 \ldots 8$.

where the vectors $\mathbf{y}$ and $\mathbf{v}$ are defined via:

$$\mathbf{y} = \begin{bmatrix} r_{1,1} \\ r_{1,2}^* \\ r_{2,1} \\ r_{2,2}^* \\ \vdots \\ r_{N_r,1} \\ r_{N_r,2}^* \end{bmatrix}, \quad \mathbf{v} = \begin{bmatrix} n_{1,1} \\ n_{1,2}^* \\ n_{2,1} \\ n_{2,2}^* \\ \vdots \\ n_{N_r,1} \\ n_{N_r,2}^* \end{bmatrix}.$$

Hence, the signal and noise components originating from different receive antennas are stacked on top of each other. The subsequent processing steps are completely analogous to the single antenna case and since:

$$\mathbf{H}_{\mathrm{v}}^H \mathbf{H}_{\mathrm{v}} = \|\mathbf{H}\|_F^2 \mathbf{I}_2$$

the resulting normalized input-output relation yields:

$$\tilde{\mathbf{s}} = \mathbf{s} + \frac{1}{\|\mathbf{H}\|_F^2} \mathbf{H}_{\mathrm{v}}^H \mathbf{v} = \mathbf{s} + \tilde{\mathbf{v}} \, .$$

The resulting noise samples are again uncorrelated:

$$\mathrm{E}\left\{\tilde{\mathbf{v}}\tilde{\mathbf{v}}^H\right\} = \frac{N_0}{\|\mathbf{H}\|_F^2}\mathbf{I}_2 \ ,$$

and the instant BER amounts to:

$$\mathrm{BER}_{\|\mathbf{H}\|_F^2} = \frac{1}{2}\mathrm{erfc}\left(\sqrt{\frac{\|\mathbf{H}\|_F^2}{2}\frac{E_b}{N_0}}\right) \ . \tag{4.15}$$

Figure 4.2 demonstrates the BER performance for $N_r = 1 \ldots 8$. By comparing (4.15) with the the ideal non-space-time coded receive diversity system (3.14) one can easily conclude that the curves in this figure are equal to the respective $2N_r$ ideal receive diversity results from Section 3.3 shifted to the right by 3dB.

4.4 Simulation Results

The organization of the following presentation of simulation results is very similar to the previous chapter. Receive and transmit selection systems are separately analyzed and the impact of receive correlation is investigated by the two endmost figures.

4.4.1 Uncorrelated Channels

Receive Selection

- **Figure 4.3** shows the results of the Alamouti STBC receive antenna selection system for $N_r = 1 \ldots 8$.
- **Figure 4.4** compares the receive selection performance with the corresponding full complexity systems for $n_r = N_r = 2, 3, 4$.

  Remarkably, the offered diversity order of $D = 2N_r$ is again equal to that of the full complexity system.
- **Figure 4.5** shows that the resulting SNR difference grows with increasing number of available receive antennas.

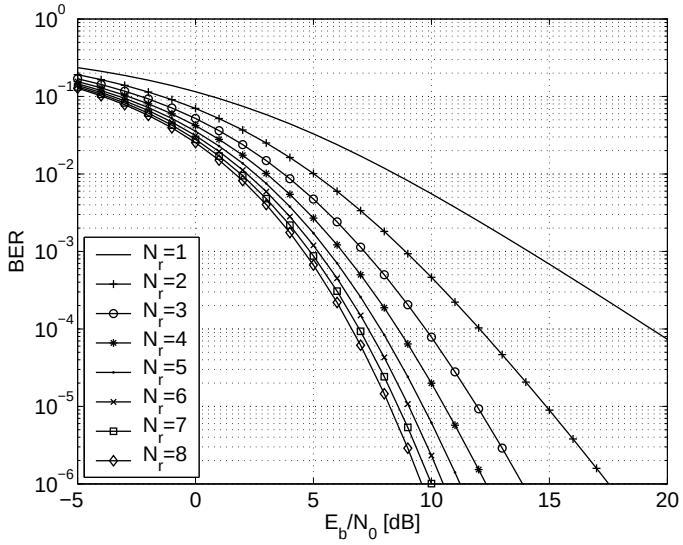

Figure 4.3: Receive selection performance using the Alamouti STBC transmission scheme and $N_r = 1 \dots 8$ available receive antennas.

Transmit Selection

- **Figure 4.6** compares the results of the Alamouti STBC transmit antenna selection system with the ideal transmit diversity system for $n_t = N_t = 2, 3, 4$. Again, they differ in average SNR by the transmit selection gain.
- **Figure 4.7** plots the transmit selection gain over the number of available transmit antennas.
- **Figure 4.8** displays the relation between b_{feedback} and obtainable transmit selection gain.

4.4.2 Correlated Channels

- **Figure 4.9** showcases the degradation of receive selection performance when the correlation at the receiver is increased from $\rho_r = 0$ to $\rho_r = 0.5, 0.75, 0.95, 1$ for the case of $N_r = 4$.
- **Figure 4.10** again demonstrates the relation between diversity and channel correlation by plotting the achievable diversity order over the number of available receive antennas with ρ_r as a parameter.

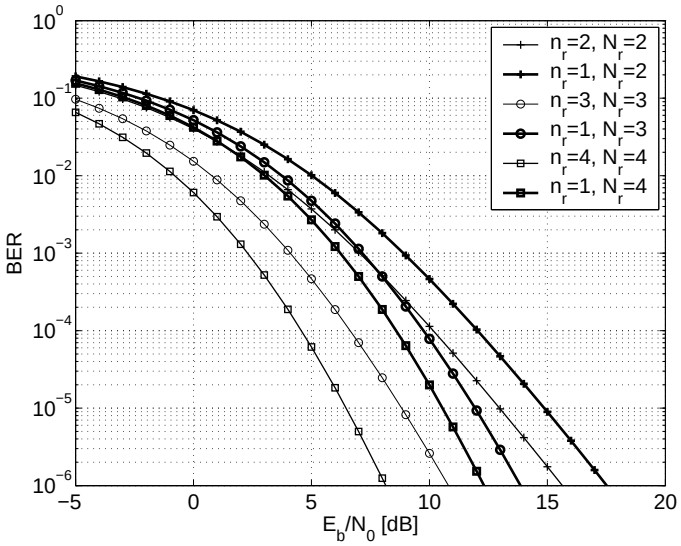

Figure 4.4: Receive selection compared to the respective full complexity systems ($n_r = N_r$) for $N_r = 2, 3, 4$.

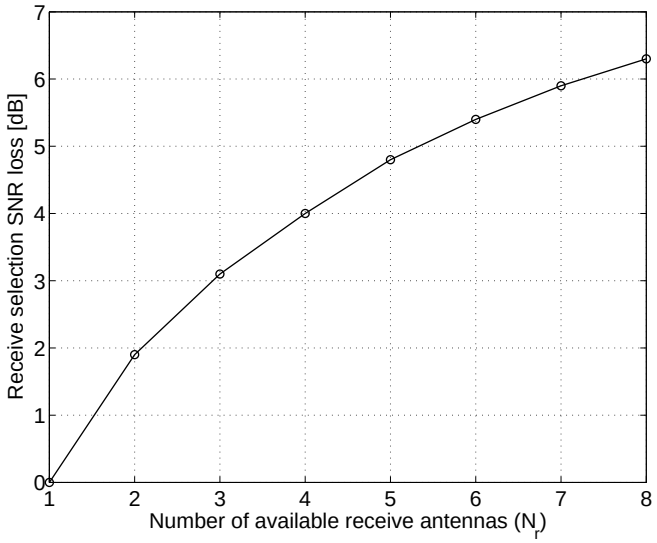

Figure 4.5: Receive selection SNR loss to the respective full complexity system, $N_r = 1 \ldots 8$.

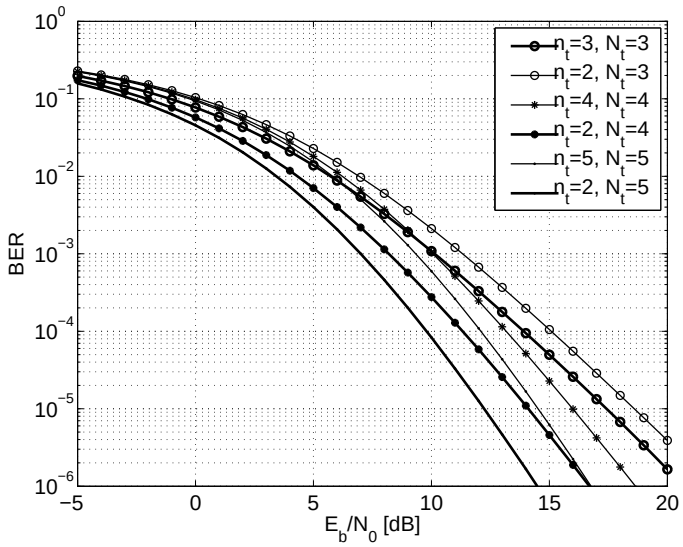

Figure 4.6: Transmit selection for $N_t = 3, 4, 5$ compared with the corresponding full complexity systems ($n_t = N_t$).

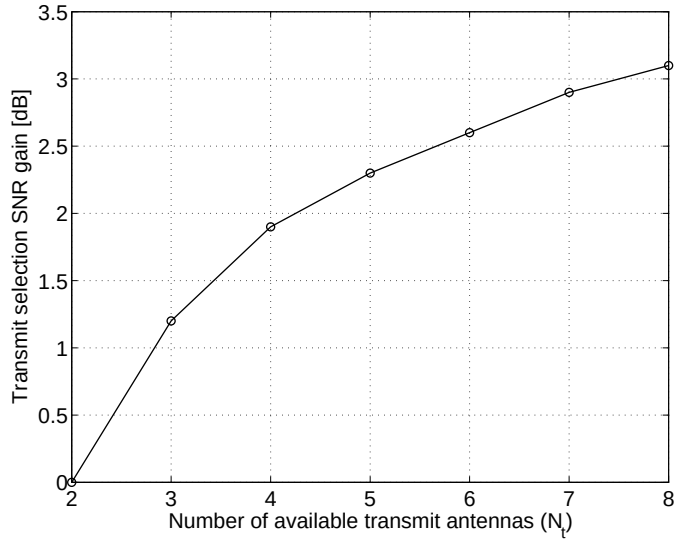

Figure 4.7: Transmit selection gain for $N_t = 2 \ldots 8$.

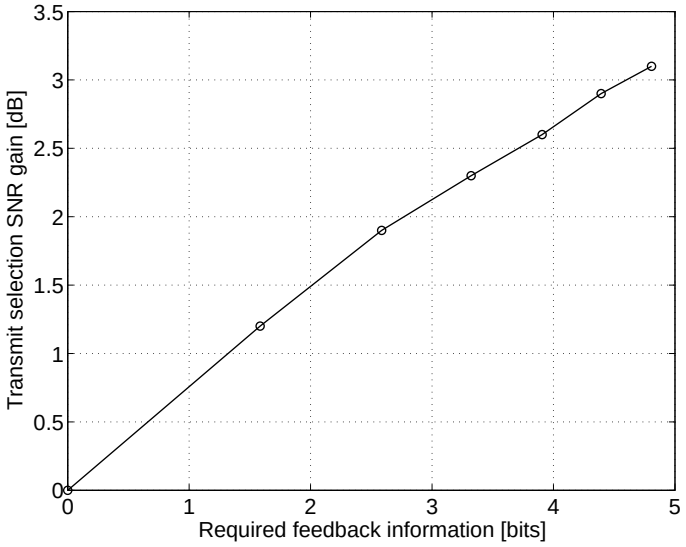

Figure 4.8: Relation between transmit selection gain and available feedback information.

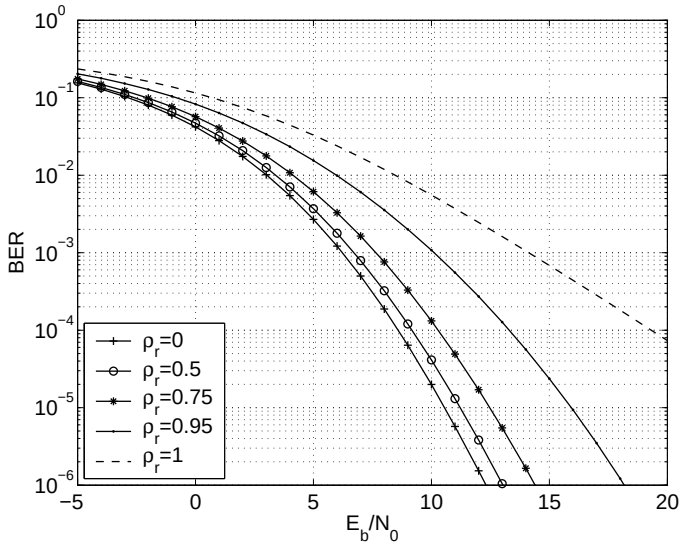

Figure 4.9: Degradation of receive selection performance in the presence of receive correlation ρ_r.

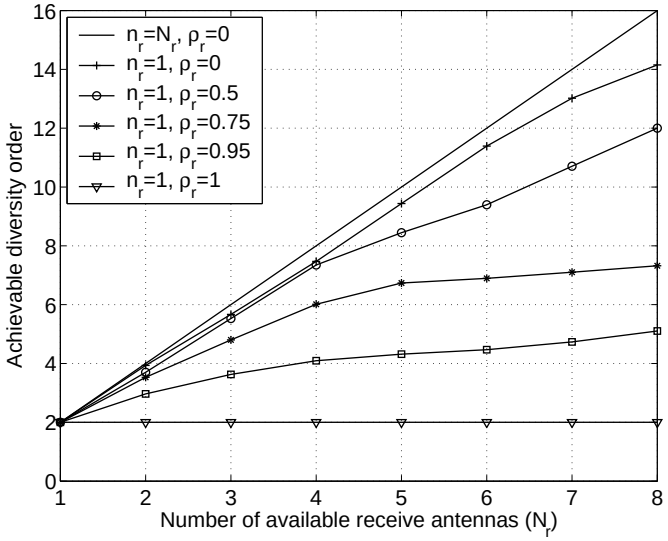

Figure 4.10: Achievable diversity order in the case of receive selection over the number of available antennas, parameterized by ρ_r.

Chapter 5

Extended Alamouti STBC

Shortly after the Alamouti scheme discussed in the previous chapter was proposed, the authors of [10] extended its functional principle to more than two transmit antennas. This led to the formulation of the theory of *generalized orthogonal designs* which is then used to construct orthogonal space-time block codes for any number of transmit antennas.

Obviously, the perfect orthogonality of a STBC is a very attractive feature since it guarantees that the offered diversity order is equal to the number of utilized transmit antennas and that simple linear detection results in optimum maximum-likelihood performance for flat fading channels.

Before getting into the details of generalized orthogonal space-time block codes an important characteristic of STBCs that has not yet been discussed in this thesis needs to be alluded, which is the rate of the code. It is defined as the number of different symbols that are encoded in the code matrix divided by the number symbol cycles that are used to transmit it. As an example the Alamouti STBC considered previously encodes two symbols in a two rowed matrix. In other words two symbols are effectively transmitted in two timeslots and so the Alamouti scheme is said to achieve the maximum possible rate of $R = 1$.

It its needless to say that a STBC that offers orthogonality in combination with full rate ($R = 1$) constitutes the optimum solution when designing codes.

Unfortunately, a theorem that has been presented and proven in [10] states that perfect orthogonality *and* maximum rate transmission is restricted to the case of two transmit antennas. This restriction is relaxed when the utilized symbol constellation is real valued only, which leads to orthogonal full rate solutions for 2,4 and 8 transmit antennas.

Given the above mentioned restrictions one could devise codes that offer perfect orthogonality with rates lower than one. An exemplary STBC presented in [10] utilizes four transmit antennas and features perfect orthogonality but only with a rate of $R = 0.75$. However, for the code that will presented in the remainder of this chapter another approach is taken.

5.1 The Extended Alamouti Scheme

This specific STBC was first proposed in [25]. It also utilizes four transmit antennas *and* offers a transmission rate of one in combination with an arbitrary complex symbol constellation. As has been mentioned above, this unavoidably means that the code cannot be perfectly orthogonal too.

So in this case the perfect orthogonality is sacrificed in order to keep the transmission rate at its maximum value of $R = 1$. As a consequence the rows and columns of the space-time code matrix (or, equivalently, the rows and columns of the virtual channel matrix) are *not* orthogonal altogether anymore.

The construction rule is easily explained since it simply consists of reiterating the Alamouti matrix construction scheme while using Alamouti structured block matrices instead of single symbols. Hence, the two matrices are generated using a total of four consecutive symbols according to:

$$\mathbf{S}_1 = \begin{bmatrix} s_1 & s_2 \\ s_2^* & -s_1^* \end{bmatrix}, \quad \mathbf{S}_2 = \begin{bmatrix} s_3 & s_4 \\ s_4^* & -s_3^* \end{bmatrix}.$$

In the second construction step these matrices are arranged to form the 4×4 space-time code matrix again realizing an Alamouti mapping:

$$\mathbf{S} = \begin{bmatrix} \mathbf{S}_1 & \mathbf{S}_2 \\ \mathbf{S}_2^* & -\mathbf{S}_1^* \end{bmatrix} = \begin{bmatrix} s_1 & s_2 & s_3 & s_4 \\ s_2^* & -s_1^* & s_4^* & -s_3^* \\ s_3^* & s_4^* & -s_1^* & -s_2^* \\ s_4 & -s_3 & -s_2 & s_1 \end{bmatrix}. \tag{5.1}$$

The input-output relation is then either formulated via:

$$\mathbf{r} = \mathbf{S}\mathbf{h} + \mathbf{n}$$

by using the corresponding (4×1) channel vector $\mathbf{h} = [h_1\, h_2\, h_3\, h_4]$ and the received signals and noise samples for four consecutive symbol cycles stacked in column vectors:

$$\mathbf{r} = \begin{bmatrix} r_1 \\ r_2 \\ r_3 \\ r_4 \end{bmatrix}, \quad \mathbf{n} = \begin{bmatrix} n_1 \\ n_2 \\ n_3 \\ n_4 \end{bmatrix}.$$

Or alternatively, by deploying the corresponding virtual channel matrix which is formed similarly by repeating the respective construction rule with two Alamouti virtual channel matrices:

$$\mathbf{H}_1 = \begin{bmatrix} h_1 & h_2 \\ -h_2^* & h_1^* \end{bmatrix} , \quad \mathbf{H}_2 = \begin{bmatrix} h_3 & h_4 \\ -h_4^* & h_3^* \end{bmatrix} ,$$

$$\mathbf{H}_\mathrm{v} = \begin{bmatrix} \mathbf{H}_1 & \mathbf{H}_2 \\ -\mathbf{H}_1^* & \mathbf{H}_1^* \end{bmatrix} = \begin{bmatrix} h_1 & h_2 & h_3 & h_4 \\ -h_2^* & h_1^* & -h_4^* & h_3^* \\ -h_3^* & -h_4^* & h_1^* & h_2^* \\ h_4 & -h_3 & -h_2 & h_1 \end{bmatrix} .$$

Thus an equivalent to (4.10) is obtained:

$$\mathbf{y} = \mathbf{H}_\mathrm{v}\mathbf{s} + \mathbf{v} , \tag{5.2}$$

with the following modified receive and noise signal vectors:

$$\mathbf{y} = \begin{bmatrix} r_1 \\ r_2^* \\ r_3^* \\ r_4 \end{bmatrix} , \quad \mathbf{v} = \begin{bmatrix} n_1 \\ n_2^* \\ n_3^* \\ n_4 \end{bmatrix} .$$

One can immediately verify that the first and the fourth as well as the second and the third row (or column respectively) of $\mathbf{H}_\mathrm{v}$ are not orthogonal to each other:

$$\mathbf{H}_\mathrm{v}^H\mathbf{H}_\mathrm{v} = \mathbf{H}_\mathrm{v}\mathbf{H}_\mathrm{v}^H = h^2 \begin{bmatrix} 1 & 0 & 0 & X \\ 0 & 1 & -X & 0 \\ 0 & -X & 1 & 0 \\ X & 0 & 0 & 1 \end{bmatrix} . \tag{5.3}$$

Here h^2 denotes the total channel gain given by the squared Frobenius norm of the MISO channel vector $\mathbf{h}$:

$$h^2 = \|\mathbf{h}\|_F^2 = |h_1|^2 + |h_2|^2 + |h_3|^2 + |h_4|^2$$

and X is defined as:

$$X = \frac{2\mathrm{Re}(h_1h_4^* - h_2h_3^*)}{h^2} . \tag{5.4}$$

Considering (5.3) the perfect orthogonality is destroyed by the channel dependent parameter X on the main skew diagonal but the remaining 8 matrix elements are strictly zero, independent of the channel vector $\mathbf{h}$. Henceforth, this code is referred to as quasi-orthogonal and X will be called the *interference parameter*.

5.1.1 ZF Receiver

Due to its non-perfect orthogonality the results using a linear receiver will clearly differ from the optimum maximum-likelihood performance. Nevertheless, the simple zero forcing (ZF) detection approach exhibits very low computational complexity and also benefits from the fact that no intricate online matrix inversion is necessary in the case of this particular code.

Similar to the analysis done for the Alamouti code in Chapter 4 the respective ZF receiver algorithm for this case is laid out by performing two successive processing steps.

The first step is the application of the matched filter $\mathbf{H}_{\mathrm{v}}^H$ on the received signal in (5.2):

$$\mathbf{z} = \mathbf{H}_{\mathrm{v}}^H\mathbf{y} = \mathbf{H}_{\mathrm{v}}^H\mathbf{H}_{\mathrm{v}}\mathbf{s} + \mathbf{H}_{\mathrm{v}}^H\mathbf{v} = \begin{bmatrix} s_1 & + & Xs_4 \\ s_2 & - & Xs_3 \\ s_3 & - & Xs_2 \\ s_4 & + & Xs_1 \end{bmatrix} + \mathbf{H}_{\mathrm{v}}^H\mathbf{v}\ .$$

Obviously, due to the interference parameter X, there remains a coupling between the symbols s_1, s_4 and s_2, s_3 which is forced to zero by the second step:

$$\tilde{\mathbf{s}} = [\mathbf{H}_{\mathrm{v}}^H\mathbf{H}_{\mathrm{v}}]^{-1}\mathbf{z} = \mathbf{s} + [\mathbf{H}_{\mathrm{v}}^H\mathbf{H}_{\mathrm{v}}]^{-1}\mathbf{H}_{\mathrm{v}}^H\mathbf{v} = \mathbf{s} + \tilde{\mathbf{v}}\ , \tag{5.5}$$

resulting in an equivalent to (4.11) or (3.2). Worded differently, the detection is realized by multiplying the received signal $\mathbf{y}$ with the Moore-Penrose pseudo-inverse of the virtual channel matrix: $[\mathbf{H}_{\mathrm{v}}^H\mathbf{H}_{\mathrm{v}}]^{-1}\mathbf{H}_{\mathrm{v}}^H$.

The correlation of the resulting filter noise samples is given by:

$$\mathrm{E}\left\{\tilde{\mathbf{v}}\tilde{\mathbf{v}}^H\right\} = \frac{N_0}{h^2(1-X^2)}\begin{bmatrix} 1 & 0 & 0 & -X \\ 0 & 1 & X & 0 \\ 0 & X & 1 & 0 \\ -X & 0 & 0 & 1 \end{bmatrix},$$

which results in two important conclusions: The power of the filtered noise increases with the interference parameter X:

$$\sigma_{\tilde{v}_i} = \frac{N_0}{h^2(1-X^2)}, \quad 1 \le i \le 4\ . \tag{5.6}$$

Secondly, the correlation between noise samples $\tilde{v}_1, \tilde{v}_4$ and $\tilde{v}_2, \tilde{v}_3$ grows even faster with increasing X which broadens the resulting performance gap to the maximum-likelihood sequence estimator.

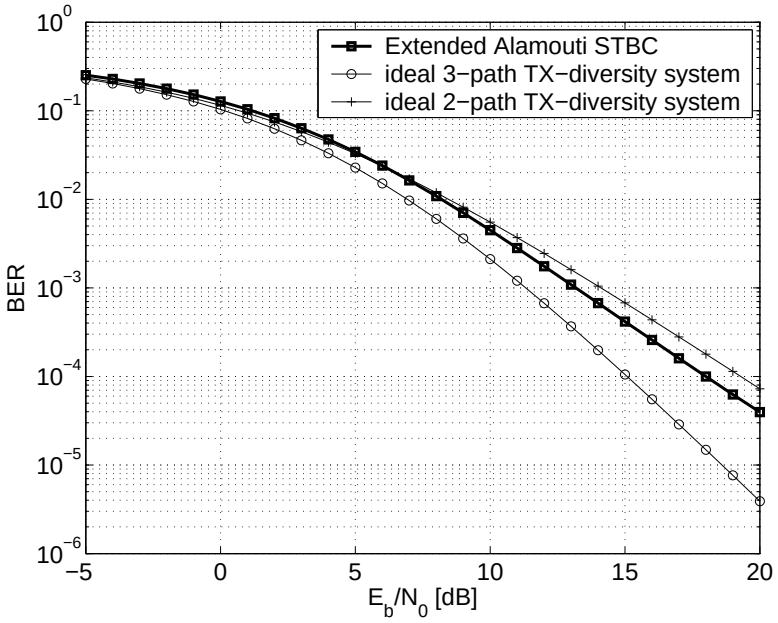

Figure 5.1: Extended Alamouti STBC performance without antenna selection using a linear ZF receiver.

Considering (5.5) and (5.6) the exact expression for the instantaneous bit error ratio is easily obtained as:

$$\mathrm{BER}_{h^2,X} = \frac{1}{2}\mathrm{erfc}\left(\sqrt{\frac{h^2(1-X^2)}{4}\frac{E_b}{N_0}}\right) . \tag{5.7}$$

The factor 4 in the denominator originates from the fact that the transmit symbols are scaled by $\frac{1}{2}$ since the total power is equally split to four transmit antennas.

Figure 5.1 shows average bit error rate progression for this (4×1) transmission scheme without any antenna selection applied. The performance is only slightly better than the original Alamouti scheme given by the ideal 2-path transmit diversity curve. The slope measurement method presented in Section 3.3.1 confirms this as it delivers an estimate for the diversity order for this system with D=2.2.

Another point of interest are the statistical properties of the channel dependent interference parameter X in the unselected case. In [26] the analytic

solution for the pdf of X is found:

$$pdf_X(\alpha) = \begin{cases} \frac{3}{4}(1-\alpha^2)\ , & \text{for} |\alpha| < 1, \\ 0\ , & \text{elsewhere.} \end{cases} \tag{5.8}$$

In the next section antenna selection will be applied and it will turn out that both the interference parameter X as well as the squared Frobenius norm of the selected MISO channel vector h^2 need to be jointly considered when computing the best antenna subset.

This presents a major drawback since the comparison of the interference parameter X for all possible antenna subsets requires the amplitudes *and* phases of all elements in the available MIMO matrix to be estimated beforehand.

5.2 Selection Criteria

5.2.1 Receive Selection

If the system is equipped with multiple receive antennas the mathematical representation of the receive selection process is given by selecting one row of the $(N_r \times 4)$ MIMO matrix:

$$\mathbf{H} = \begin{bmatrix} h_{11} & h_{12} & h_{13} & h_{14} \\ h_{21} & h_{22} & h_{23} & h_{24} \\ \vdots & \vdots & \vdots & \vdots \\ h_{N_r1} & h_{N_r2} & h_{N_r3} & h_{N_r4} \end{bmatrix} \quad \rightarrow \quad \mathbf{h}_i = \begin{bmatrix} h_{i1} & h_{i2} & h_{i3} & h_{i4} \end{bmatrix} .$$

In the following three specific variants are analyzed:

Maximization of the Channel Gain:

$$i = \underset{1 \le i \le N_r}{\arg\max}\ h_i^2 = \underset{1 \le i \le N_r}{\arg\max} \left(|h_{i1}|^2 + |h_{i2}|^2 + |h_{i3}|^2 + |h_{i4}|^2 \right) . \tag{5.9}$$

Minimization of Interference Parameter X:

$$i = \underset{1 \le i \le N_r}{\arg\min} |X_i| = \underset{1 \le i \le N_r}{\arg\min} \left(\frac{2|\mathrm{Re}(h_{i1}h_{i4}^* - h_{i2}h_{i3}^*)|}{h_i^2} \right) . \tag{5.10}$$

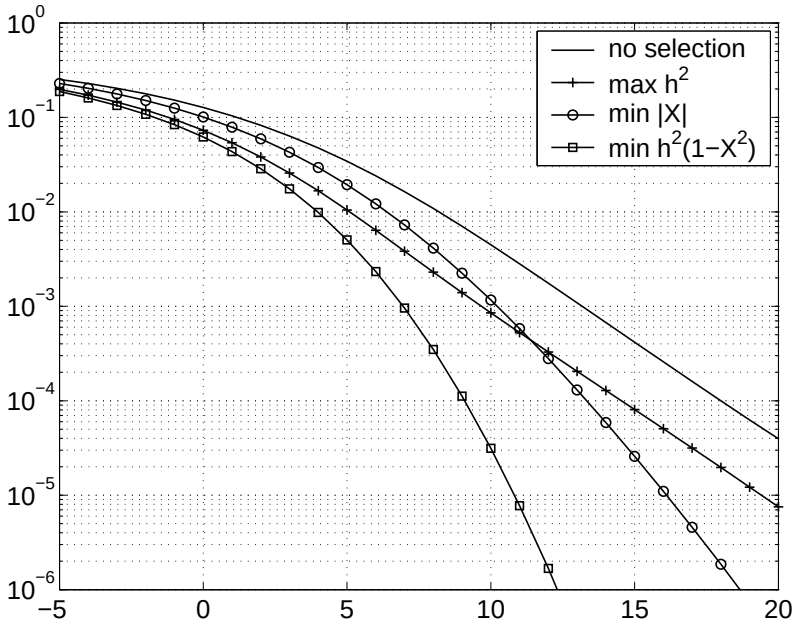

Figure 5.2: Comparison of various receive selection strategies for $N_r = 4$.

Minimization of Filtered Noise Power:

$$i = \underset{1 \le i \le N_r}{\arg\max} \left[h_i^2 (1 - X_i^2) \right] \ . \tag{5.11}$$

Figure 5.2 compares the resulting system performances for all three variants when $N_r = 4$ receive antennas are available to choose from. As expected, the minimization of the filtered noise delivers the best results, as it also directly minimizes the instant BER as given by (5.7).

Remarkably, the exclusive maximization of $\|\mathbf{h}\|_F^2$ does not increase the diversity but offers a 3.4dB gain in average SNR only. This is explained easily since this algorithm completely neglects the value of X for the selected row of the MIMO matrix. Simulations showed that when applying the $\min |X|$ algorithm the system performance for the case of $N_r = 4$ cannot be further improved noticeably by adding additional receive antennas to choose from. This justifies the conclusion that this selection algorithm is reducing the mean of X very efficiently. Unfortunately, since the statistics of h^2 do not change at all when applying this criteria, the resulting system cannot outperform an ideal 4-path transmit diversity scheme, no matter how many receive antennas are available.

Figure 5.3 confirms the aforementioned propositions by displaying the histograms of $|X|$ for all three algorithms for $N_r = 4$. Note the relatively

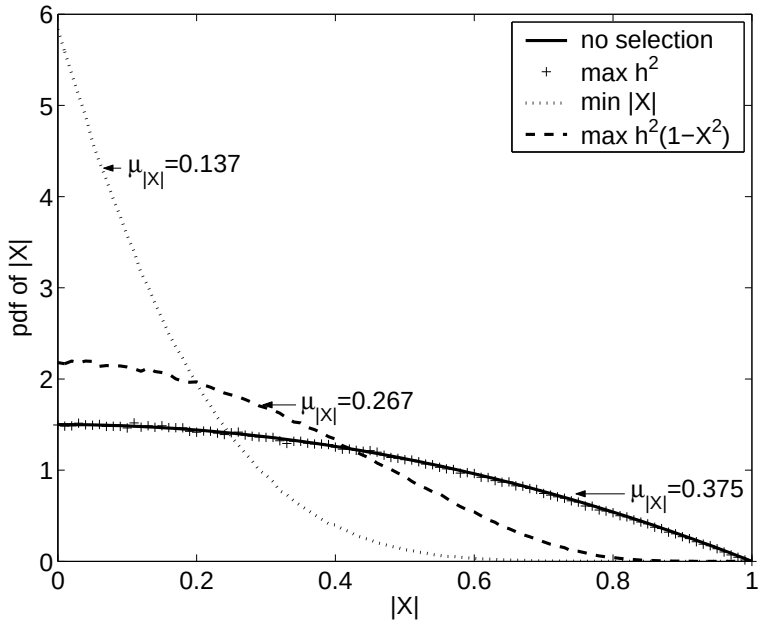

Figure 5.3: Histogram of the resulting interference parameter X after applying receive antenna selection, $N_r = 4$.

large resulting mean of $|X|$ when the optimum antenna selection algorithm is used.

5.2.2 Transmit Selection

The previous case of receive selection showed that maximization of the selected channel Frobenius norm delivers very poor results since the current value of X has *considerable* impact on the instant bit error ratio and must not be neglected when computing the optimum receive antenna.

Now the closed loop transmit selection case is considered. The applied antenna switch connects each of the four encoded space-time symbol streams to one specific transmit antenna. Obviously, this multiplexer also determines which symbol stream (column of the space-time code matrix) is connected to which selected transmit antenna.

Since swapping the coefficients in (5.4) leads to different values of $|X|$ the possibility of changing the assignment of symbol streams to the antenna elements (reordering) provides an additional degree of freedom. Given a selected set of four antennas, it is easily shown that the total of 24 permutations can be broken down into three groups. The 8 permutations constituting one

group all exhibit the same absolute value of $|X|$. It follows that there exist only three distinct values of $|X|$ for a set of 4 already selected channel coefficients when reordering is allowed:

- $|X_{i,j,k,l}|$ Original order
- $|X_{k,j,i,l}|$ First and third element swapped
- $|X_{i,l,k,j}|$ Second and fourth element swapped

If, in addition to the indices of the selected antennas, the best out of these three ordering variants is communicated to the transmitter via the feedback link the resulting $|X|$ will be smaller than when no swapping is done and only the default order is used.

The question that arises is if the gained decrease of the instantaneous BER is really worth the additional amount of feedback information. Or, worded differently, do the statistics of $|X|$ improve *significantly* when the swapping of antennas is allowed at the transmitter. The next few subsections will elaborate on this subject.

5.2.3 Standard Transmit Antenna Selection

Starting point is the original transmit antenna selection system equipped with $N_t > 4$ transmit antennas and no reordering capability:

$$\mathbf{h} = \begin{bmatrix} h_1 \\ h_2 \\ \vdots \\ h_{N_t} \end{bmatrix} \quad \rightarrow \quad \mathbf{h}_{i,j,k,l} = \begin{bmatrix} h_i \\ h_j \\ h_k \\ h_l \end{bmatrix}, \quad 1 \leq i < j < k < l \leq N_t \; .$$

The selection process consists of selecting four antennas out of N_t available ones and the ordering of antenna elements is always set to the default sequence with strictly increasing indices. Again, the following three already presented variants are distinguished:

Maximization of the Channel Gain:

$$i, j, k, l = \underset{1 \leq i < j < k < l \leq N_t}{\arg\max} \left(|h_i|^2 + |h_j|^2 + |h_k|^2 + |h_l|^2 \right) \; .$$

Minimization of Interference Parameter X:

$$i, j, k, l = \underset{1 \leq i < j < k < l \leq N_t}{\arg\min} \left(\frac{2|\mathrm{Re}(h_i h_l^* - h_j h_k^*)|}{h_{i,j,k,l}^2} \right) \; . \tag{5.12}$$

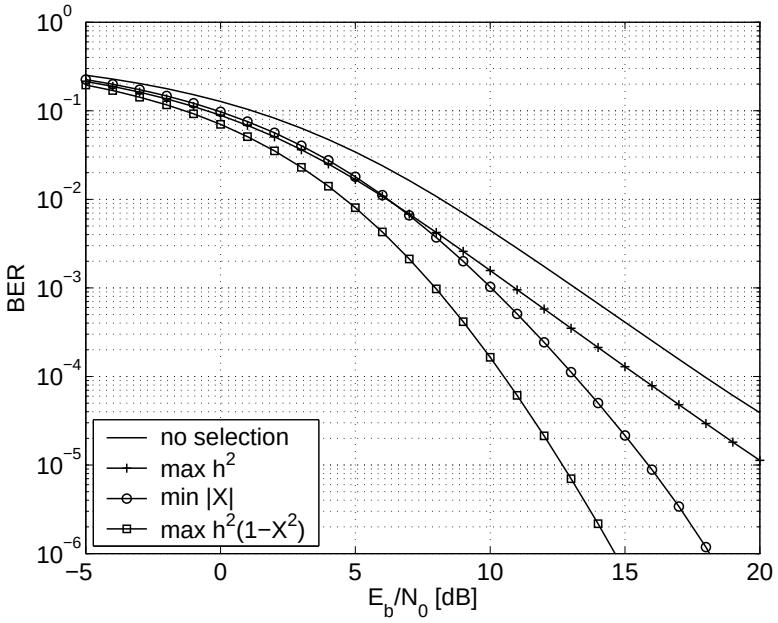

Figure 5.4: Comparison of various transmit selection strategies for $N_t = 6$ with no reordering applied.

Minimization of Filtered Noise Power:

$$i, j, k, l = \underset{1 \le i < j < k < l \le N_t}{\arg\max} \left[h_{i,j,k,l}^2 (1 - X_{i,j,k,l}^2) \right] \ . \tag{5.13}$$

The results are depicted in Figure 5.4 and matters are shown to be very similar to the receive selection case. Again, the maximization of the squared Frobenius norm delivers very poor results and does not increase the diversity order.

Obviously, the number of effectively different subsets equals the number of possibilities to combine four out of N_t elements without observing order:

$$q_{\text{eff}} = \binom{N_t}{4} \ ,$$

which results in a feedback bit length of:

$$b_{\text{feedback}} = \log_2(q_{\text{eff}}) = \log_2 \left[\binom{N_t}{4} \right] \ .$$

5.2.4 Transmit Antenna Selection with Reordering Capability

Now the two algorithms (5.12) and (5.13) that incorporate the interference parameter in their respective criterion are applied in combination with the selection of one out of the three possible ordering options:

$$\mathbf{h} = \begin{bmatrix} h_1 \\ h_2 \\ \vdots \\ h_{N_t} \end{bmatrix} \quad \rightarrow \quad \mathbf{h}_{i,j,k,l} = \begin{bmatrix} h_i \\ h_j \\ h_k \\ h_l \end{bmatrix}, \; \mathbf{h}_{k,j,i,l} = \begin{bmatrix} h_k \\ h_j \\ h_i \\ h_l \end{bmatrix}, \; \mathbf{h}_{i,l,k,j} = \begin{bmatrix} h_i \\ h_l \\ h_k \\ h_j \end{bmatrix} .$$

Minimization of Interference Parameter X:

Here, the best antenna subset with the smallest value of $|X|$ for each of the three ordering possibilities is computed. The subsequent comparison of the three resulting values leads to final selection of the subset/ordering combination that offers the smallest value of $|X|$.

$$\begin{aligned} |X_1| &= \min_{1\leq i<j<k<l\leq N_t} |X_{i,j,k,l}| \, , \\ |X_2| &= \min_{1\leq i<j<k<l\leq N_t} |X_{k,j,i,l}| \, , \\ |X_3| &= \min_{1\leq i<j<k<l\leq N_t} |X_{i,l,k,j}| \, , \end{aligned}$$

$$m = \arg\min_{1\leq m\leq 3} |X_m| \, .$$

Minimization of Filtered Noise Power:

Again the three permutation variants are considered separately:

$$\begin{aligned} p_1 &= \min_{1\leq i<j<k<l\leq N_t} h_{i,j,k,l}^2 (1 - X_{i,j,k,l}^2) \, , \\ p_2 &= \min_{1\leq i<j<k<l\leq N_t} h_{i,j,k,l}^2 (1 - X_{k,j,i,l}^2) \, , \\ p_3 &= \min_{1\leq i<j<k<l\leq N_t} h_{i,j,k,l}^2 (1 - X_{i,l,k,j}^2) \, , \end{aligned}$$

and the optimum subset/order configuration is obtained by:

$$m = \arg\min_{1\leq m\leq 3} |p_m| \, .$$

For both algorithms, the number of effectively different subsets is thrice as high as for the standard transmit selection:

$$q_{\text{eff}} = 3\binom{N_t}{4} .$$

Consequently, the required feedback bit length is increases to:

$$b_{\text{feedback}} = \log_2\left[3\binom{N_t}{4}\right] = \log_2\left[\binom{N_t}{4}\right] + 1.585 .$$

5.2.5 Additional Code Selection Approaches

An alternative way of improving the statistics of X and thereby enhancing the performance of the resulting closed loop system is the application of code selection as proposed in [17]. Here, the feedback link is utilized to select one out of a small set of available STBCs which is then used for transmission. These STBCs are all similarly structured and exhibit the same instantaneous bit error ratio as it has been given by (5.7) but with a differently defined interference parameter X.

As an example, by changing the sign of every occurrence of s_2 in the space-time code matrix $\mathbf{S}$ (5.1) a variant of the extended Alamouti code presented at the beginning of this chapter is obtained:

$$\mathbf{S} = \begin{bmatrix} s_1 & -s_2 & s_3 & s_4 \\ -s_2^* & -s_1^* & s_4^* & -s_3^* \\ s_3^* & s_4^* & -s_1^* & s_2^* \\ s_4 & -s_3 & s_2 & s_1 \end{bmatrix} . \tag{5.14}$$

The bit error ratio for the ZF receiver is again equal to (5.7) whereas the corresponding definition of the interference parameter X changes to:

$$X = \frac{2\text{Re}(h_1 h_4^* + h_2 h_3^*)}{h^2} .$$

Note that this specification of X is not obtainable by changing the order of coefficients in the original definition of X in (5.4). Hence, additional code selection capability is expected to further lower the minimum value of $|X|$ that is achievable for a given channel realization by means of selection and reordering alone.

The resulting system under consideration is capable of:

- selecting coefficients h_i, h_j, h_k, h_l out of the MISO channel vector $\mathbf{h} = [h_1\, h_2\, \ldots\, h_{N_t}]$,

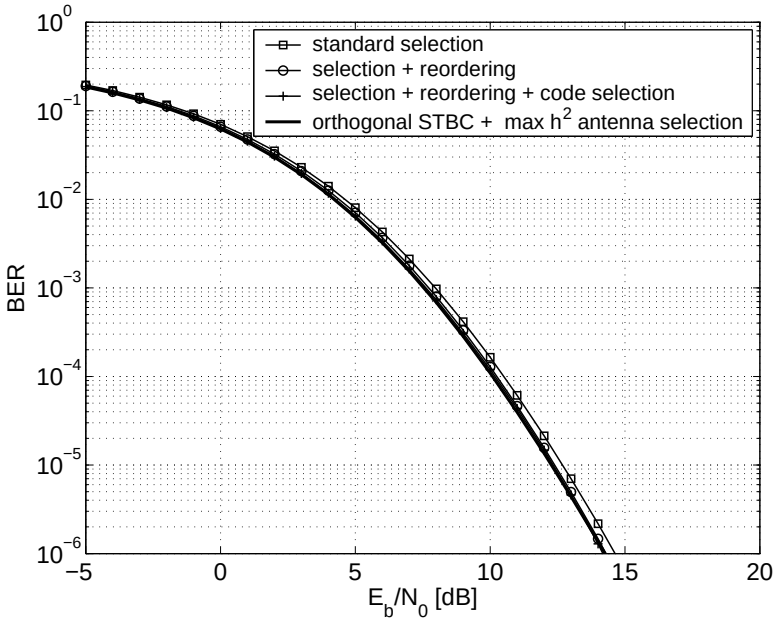

Figure 5.5: Extended transmit selection variants compared for $N_t = 6$.

- changing the order to either h_k, h_j, h_i, h_l or h_i, h_l, h_k, h_j and
- applying one of the available STBCs given by (5.1) and (5.14).

This further complicates the selection process as the algorithms outlined in subsection 5.2.4 need to be repeated for each of the two available code variants. Additionally, the amount of required feedback information also increases to:

$$b_{\text{feedback}} = \log_2 \left[\binom{N_t}{4} \right] + 2.585 \; .$$

After having established two ways to enhance the standard transmit selection scheme (in subsection 5.2.4 and 5.2.5) a final performance comparison needs to be done in order to assess if the additional degrees of freedom (and the corresponding bits of feedback information) are exploited efficiently.

Unfortunately, considering Figure 5.5 it shows that the achievable performance gains are negligible. A total of 0.3dB is gained by the reordering approach and the code-selection gain is hardly measurable. On the other hand, this comes at no surprise since the bold curve in Figure 5.5 shows the analytically obtained performance of a non-full rate, perfect orthogonal

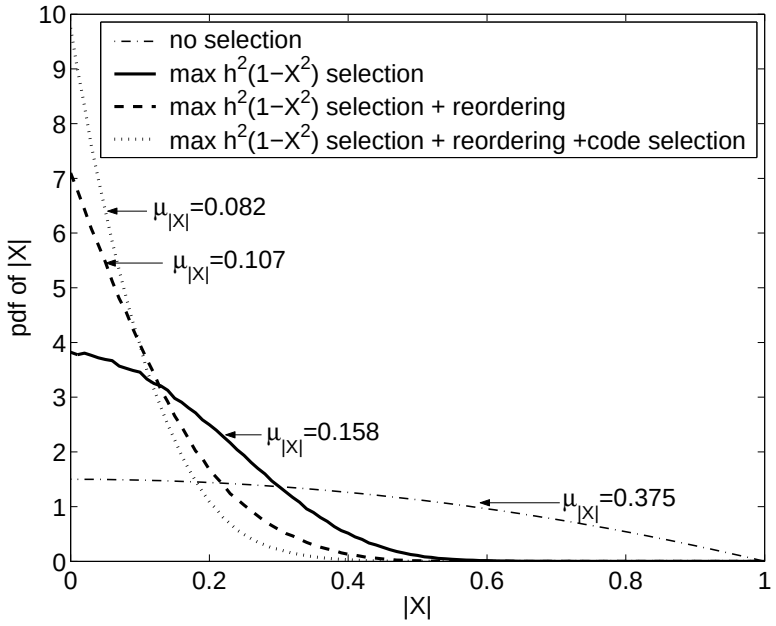

Figure 5.6: Histogram of the resulting interference parameter $|X|$ after applying extended transmit selection algorithms, $N_t = 6$.

(4×1) STBC in combination with antenna selection (maximizing the Frobenius norm). This system equals the case when the interference parameter is effectively *zero* all the time and specifies a reference result that cannot be outperformed, no matter how many additional degrees of freedom are available to reduce $|X|$.

Finally, Figure 5.6 provides further insight into to this subject since it illustrates how the statistical properties of $|X|$ change after incorporating additional reordering and code switching capabilities. The solid line corresponds to the standard transmit selection and the dotted line depicts the results with applied reordering *and* code selection. Interestingly, the clear difference between these two histograms only amounts to a very small gain in performance (0.3 dB) as has been shown in Figure 5.5.

5.3 Reference Systems

Similarly to the previous chapters, the respective receive selection system performance is assessed by direct comparison with the full complexity case $(n_r = N_r)$. The instant BER for these maximum ratio receive combining

schemes is obtained as follows:

The elements in the individual rows of total MIMO channel matrix given by:

$$\mathbf{H} = \begin{bmatrix} h_{11} & h_{12} & h_{13} & h_{14} \\ h_{21} & h_{22} & h_{23} & h_{24} \\ \vdots & \vdots & \vdots & \vdots \\ h_{N_r1} & h_{N_r2} & h_{N_r3} & h_{N_r4} \end{bmatrix} , \tag{5.15}$$

are used to generate N_r virtual channel sub-matrices:

$$\mathbf{H}_n = \begin{bmatrix} h_{n1} & h_{n2} & h_{n3} & h_{n4} \\ -h_{n2}^* & h_{n1}^* & -h_{n4}^* & h_{n3}^* \\ -h_{n3}^* & -h_{n4}^* & h_{n1}^* & h_{n2}^* \\ h_{n4} & -h_{n3} & -h_{n2} & h_{n1} \end{bmatrix} \quad , \quad 1 \leq n \leq N_r \ ,$$

and stacking those 4×4 matrices on top of each other finally yields the correct virtual channel matrix for the extended Alamouti transmission scheme with N_r receive antennas:

$$\mathbf{H}_{\mathrm{v}} = \begin{bmatrix} \mathbf{H}_1 \\ \mathbf{H}_2 \\ \vdots \\ \mathbf{H}_{N_r-1} \\ \mathbf{H}_{N_r} \end{bmatrix} .$$

The receive processing steps are completely analogous to the single receive antenna case and the resulting exact expression of the instantaneous bit error ratio works out to:

$$\mathrm{BER}_{h^2,X} = \frac{1}{2}\mathrm{erfc}\left(\sqrt{\frac{h^2(1-X^2)}{4}\frac{E_b}{N_0}}\right) .$$

where h^2 is now equal to the squared Frobenius norm of the total channel MIMO matrix (5.15):

$$h^2 = \|\mathbf{H}\|_F^2 = \sum_i^{N_r} |h_{i1}|^2 + |h_{i2}|^2 + |h_{i3}|^2 + |h_{i4}|^2 \ ,$$

and the definition of the interference parameter changes to:

$$X = \sum_i^{N_r} \frac{2\mathrm{Re}(h_{i1}h_{i4}^* - h_{i2}h_{i3}^*)}{h^2} \ , \tag{5.16}$$

Figure 5.7 shows the respective simulation results for $N_r = 1 \ldots 8$.

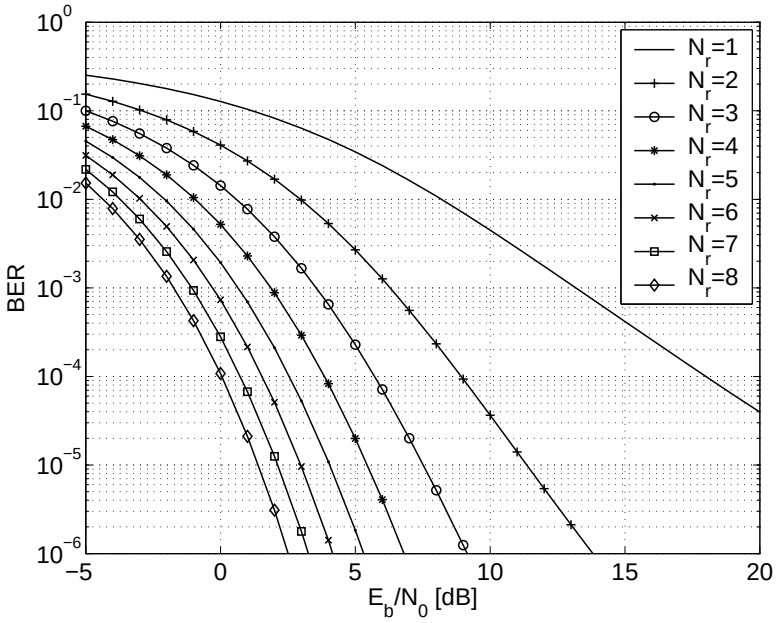

Figure 5.7: Extended Alamouti STBC transmission system utilizing multiple receive antennas, $N_r = 1 \dots 8$.

5.4 Simulation Results

Finally, this chapter is concluded by the numerical simulation figures again presenting the same collection of results and comparisons as was done in the two preceding chapters.

5.4.1 Uncorrelated Channels

Receive Selection

- **Figure 5.8** shows the results of the receive antenna selection system for $N_r = 1 \dots 8$ applying the optimum receive selection criterion.
- **Figure 5.9** compares the receive selection performance for $N_r = 2, 3, 4$ with the corresponding full complexity systems $n_r = N_r = 2, 3, 4$.

  Again, the diversity gain of the full complexity system is maintained by the single receive antenna selection scheme.
- **Figure 5.10** shows the progression of the resulting SNR loss.

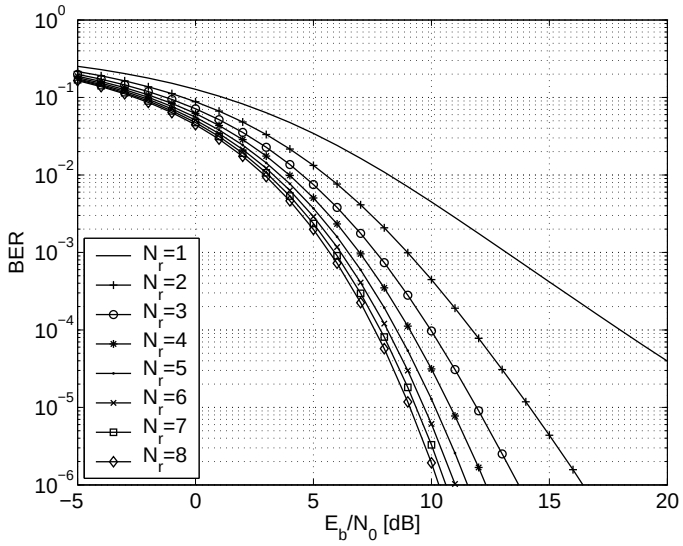

Figure 5.8: Extended Alamouti receive selection system using the optimum $max\ h^2(1-X^2)$ criterion, $N_r = 1 \ldots 8$.

Transmit Selection

- **Figure 5.11** compares the results of the extended Alamouti STBC transmit antenna selection system (optimum criterion without reordering and code selection) with the ideal transmit diversity system for $n_t = N_t = 5, 6, 7$.
- **Figure 5.12** plots the resulting selection gain over the number of available transmit antennas.
- **Figure 5.13** displays the relation between b_{feedback} and transmit selection SNR gain.

5.4.2 Correlated Channels

Finally, **Figure 5.14** demonstrates the performance degradation of the receive selection scheme when receiver side channel correlation is gradually increased for $N_r = 4$ available receive antennas.

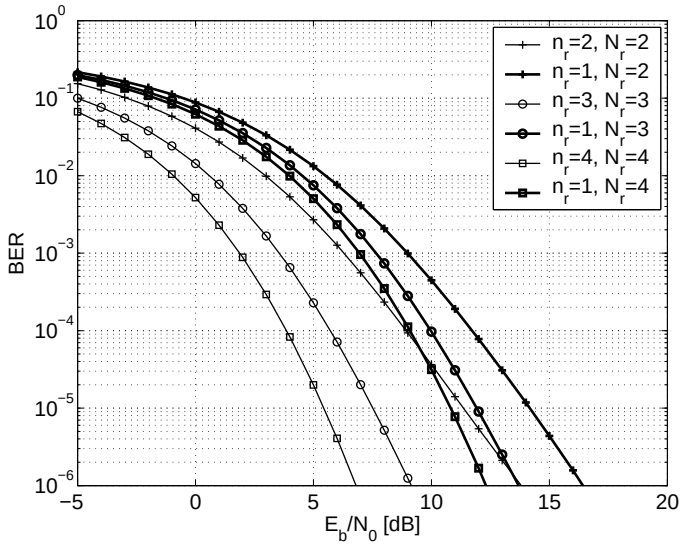

Figure 5.9: Comparison of receive selection performance with the respective full complexity MRRC schemes.

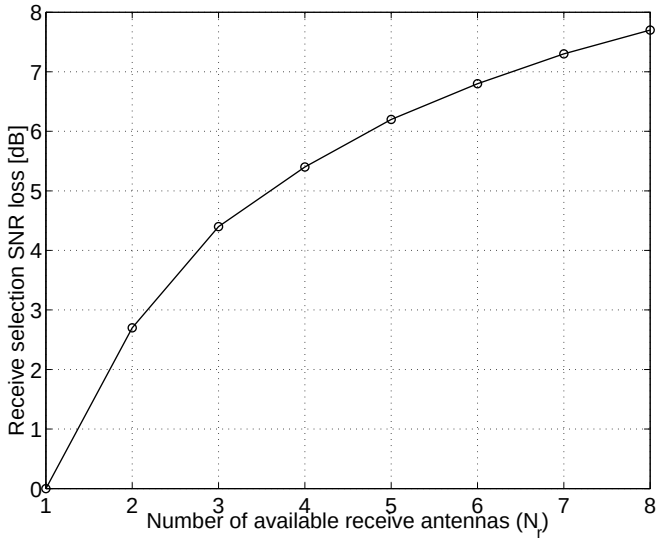

Figure 5.10: Resulting average SNR loss over the number of available receive antennas.

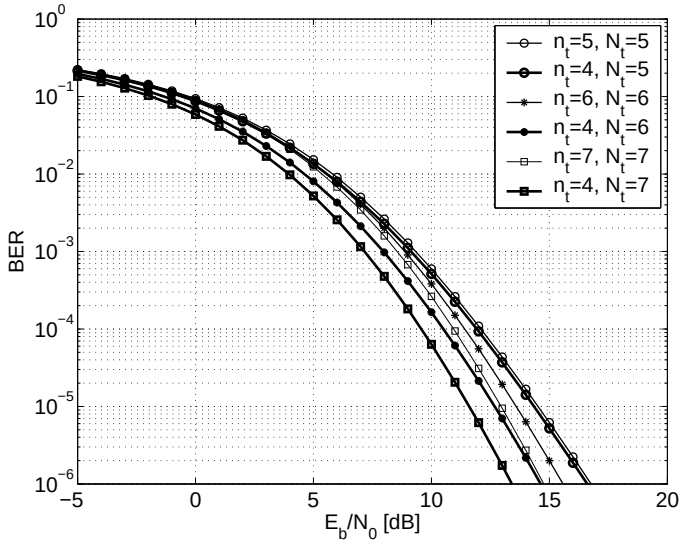

Figure 5.11: Transmit selection performance for $N_t = 5, 6, 7$ using the $max\ h^2(1-X^2)$ criterion (without reordering and code selection extensions), compared with the corresponding ideal transmit diversity systems.

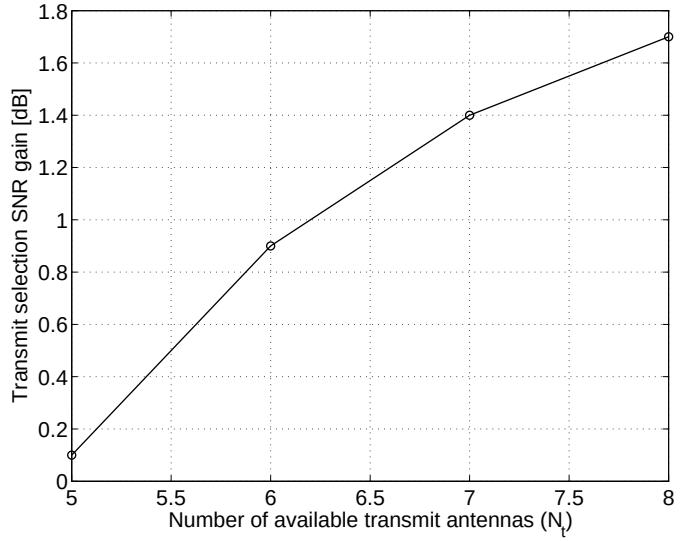

Figure 5.12: Progression of transmit selection gain with an increasing number of available transmit antennas.

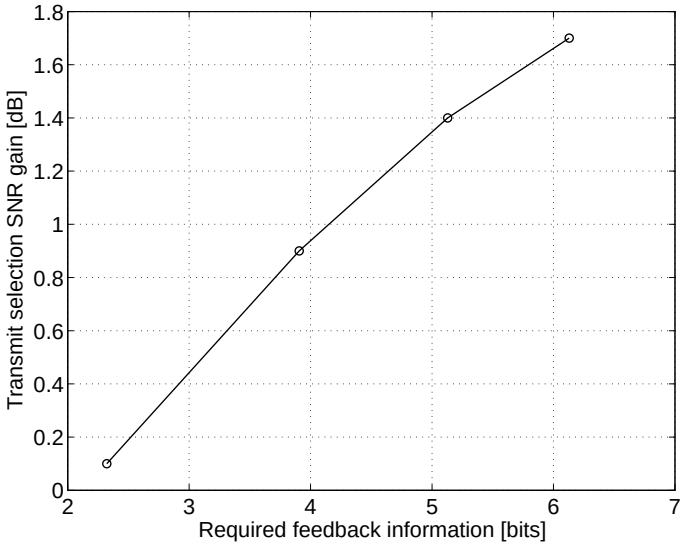

Figure 5.13: Interrelation of closed loop transmit selection gain and required amount of feedback information.

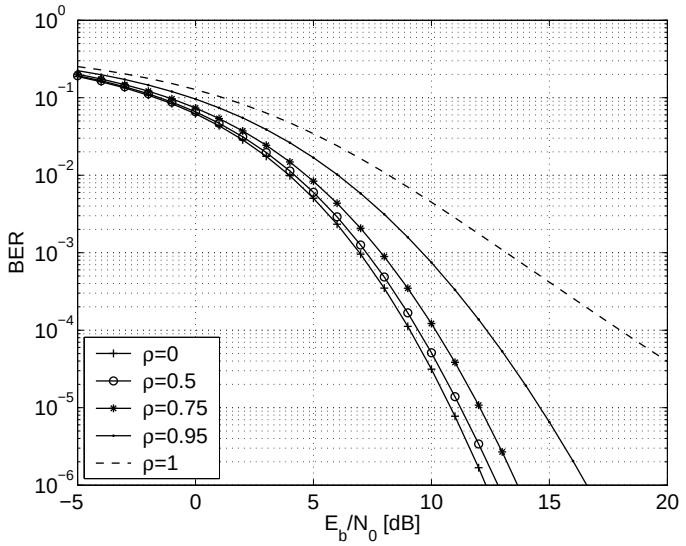

Figure 5.14: Receive selection performance (applying the optimum criterion) when channel correlation is introduced, $N_r = 4$.

Chapter 6

Summary and Conclusion

The three preceding chapters were dedicated to the rigorous analysis of three different transmission techniques in combination with transmit and receive antenna selection. In this final chapter an attempt to work out the most important differences in terms of respective antenna selection performance will be made.

One important question seems to be: Does it really offer a considerable benefit if space-time coding is combined with antenna selection, or is it more advisable to apply the selection principle to systems that only utilize a single antenna for transmission?

The correct answer in the case of receive selection is easily concluded by observing Figure 6.1 as it clearly demonstrates that the application of space-time coding in combination with receive antenna selection is enhancing the diversity of the system significantly. When less than four antennas are available to choose from one can expect that the Alamouti transmission scheme almost doubles the respective diversity order that is obtainable with the non-space-time coded single antenna system. Note that the differences would be even more pronounced if no channel correlation was present.

On the other hand, one cannot extend this corollary to the case of transmit selection. Figure 6.2 shows that under the assumption that the number of available transmit antennas is kept fixed at $N_t = 6$ the extended as well as the standard Alamouti transmission system is outperformed by the single antenna scheme in terms of average SNR.

This can be explained as follows: Basically, the closed loop approach allows to assign the transmit power onto the antenna that exhibits the lowest attenuation (i.e. highest path gain) to the receive antenna. If the number of simultaneously used transmit antennas is increased to two by applying the Alamouti scheme the total transmit power is then equally split on the best

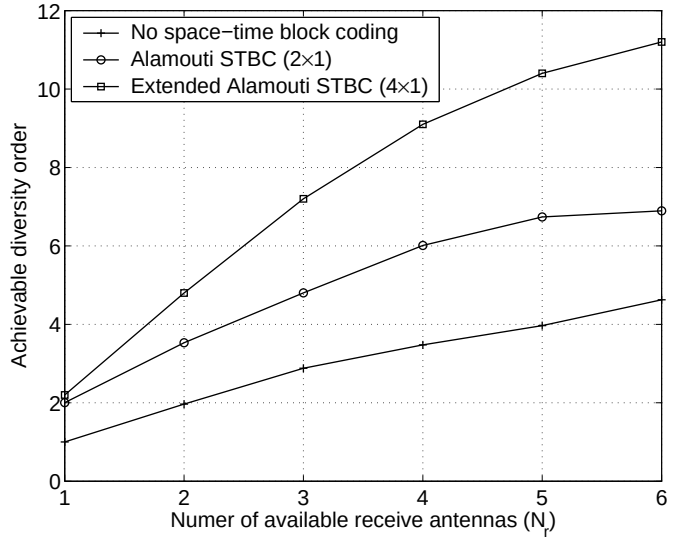

Figure 6.1: Achievable diversity order for the three considered transmission techniques applying receive antenna selection in correlated channels, $\rho_r = 0.75$.

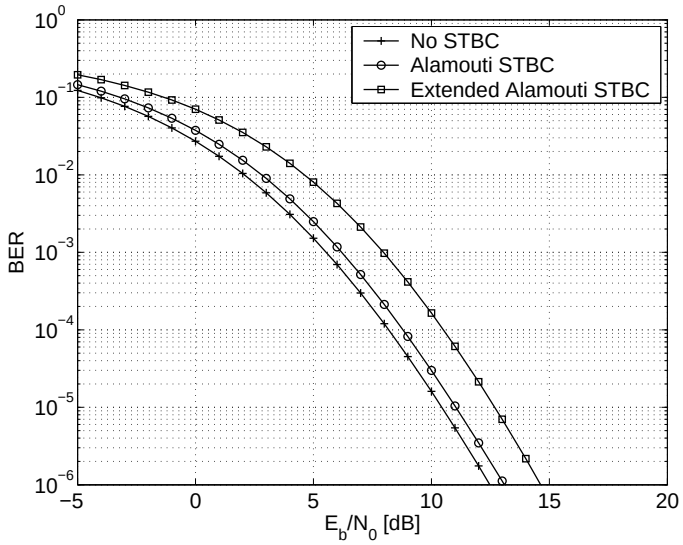

Figure 6.2: Transmit selection performance for the three considered transmission schemes, $N_t = 6$.

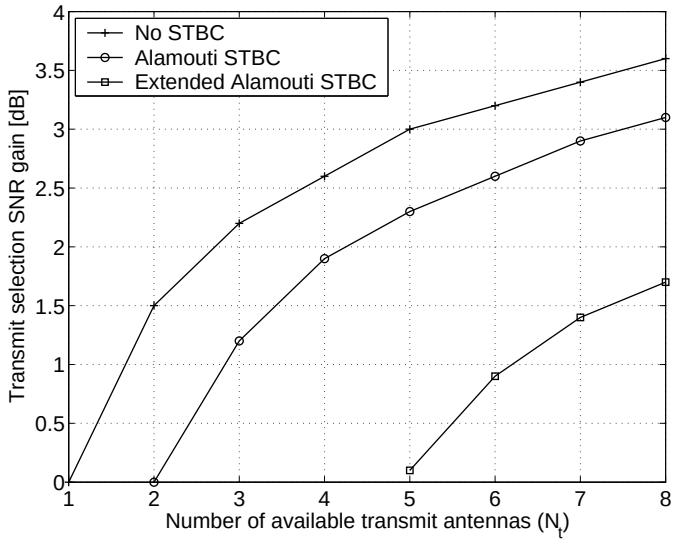

Figure 6.3: Comparison of the transmit selection gain.

and the second best antenna. This amounts to the loss of average SNR that is visible in Figure 6.2 and matters become even worse when the extended Alamouti scheme is used. Figure 6.3 also confirms this as it shows that the transmit selection gains are *decreasing* as soon as a STBC scheme is applied.

Hence, the fundamental conclusion is: Closed loop transmit selection performs best when **not** combined with space-time block coding. Note that this implication is based on the following assumptions (c.f. Chapter 2):

- Quasi-static channel
- Perfect channel estimation
- Ideal feedback link (errorfree, zero-latency)

As a final remark a simulation result with deliberately introduced feedback errors is presented. Figure 6.4 impressively shows that the performance of the non-space-time coded transmit selection system completely deteriorates, whereas both STBC based schemes are still able do deliver reasonable transmit diversities.

It is conjectured that this behavior becomes even more distinct when the remaining two idealistic model assumptions are also replaced by more realistic ones (e.g. frequent channel estimation errors, continuous fading model instead of block fading).

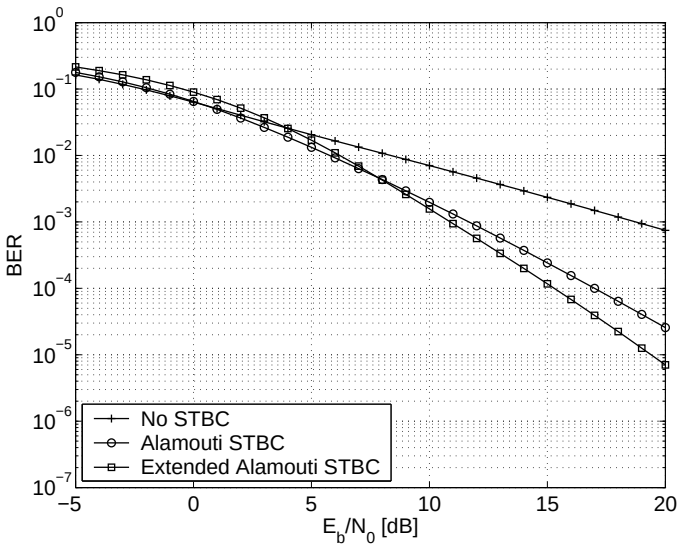

Figure 6.4: Transmit selection performance when a constant feedback link bit error ratio of $\mathrm{BER}_{\mathrm{feedback}} = 10^{-2}$ is assumed.

Bibliography

[1] J.H. Winters, "On the Capacity of Radio Communication Systems with Diversity in a Rayleigh Fading Environment," *IEEE Journal on Selected Areas in Communications*, Volume: 5, Issue: 5, Pages: 871 - 878, June 1987.

[2] G.J. Foschini and M.J. Gans, "On Limits of Wireless Communications in Fading Environments when Using Multiple Antennas," *Wireless Personal Communications*, Volume: 6, Pages: 311 - 335, March 1998.

[3] I.E. Telatar, "Capacity of Multi-Antenna Gaussian Channels," *European Transactions on Telecommunications*, Volume: 10, Issue: 6, Pages: 585 - 595, Dec 1999.

[4] A.J. Paulraj, D.A Gore, R.U. Nabar and H. Bölcskei, "An Overview of MIMO Communications - A Key to Gigabit Wireless," *Proceedings of the IEEE*, Volume: 92, Issue: 2, Pages: 198 - 218, Feb. 2004.

[5] J.H. Winters, "The Diversity Gain of Transmit Diversity in Wireless Systems with Rayleigh Fading," *IEEE Transactions on Vehicular Technology*, Volume: 47, Issue: 1, Pages: 119 - 123, Feb. 1998.

[6] V. Tarokh, N. Seshadri and A.R. Calderbank, "Space-Time Codes for High Data Rate Wireless Communication: Performance Criterion and Code Construction," *IEEE Transactions on Information Theory*, Volume: 44, Issue: 2, Pages: 744 - 765, March 1998.

[7] D. Gesbert, M. Shafi, Da-shan Shiu, P.J. Smith and A. Naguib, "From Theory to Practice: An Overview of MIMO Space-Time Coded Wireless Systems," *IEEE Journal on Selected Areas in Communications*, Volume: 21, Issue: 3, Pages: 281 - 302, April 2003

[8] A. Hottinen, O. Tirkkonen and R. Wichman, *Multi-Antenna Transceiver Techniques for 3G and Beyond*, Wiley, 2003

[9] V. Tarokh, H. Jafarkhani and A.R. Calderbank, "Space-Time Block Coding for Wireless Communications: Performance Results," *IEEE Journal on Selected Areas in Communications*, Volume: 17, Issue: 3, Pages:451 - 460, March 1999

[10] V. Tarokh, H. Jafarkhani and A.R. Calderbank, "Space-Time Block Codes from Orthogonal Designs," *IEEE Transactions on Information Theory*, Volume: 45, Issue: 5, Pages: 1456 - 1467, July 1999

[11] S. Sandhu, R. Heath and A. Paulraj, "Space-Time Block Codes Versus Space-Time Trellis Codes," *IEEE International Conference on Communications, 2001*, Volume: 4, Pages: 1132 - 1136, June 2001

[12] A.F. Molisch and M.Z. Win, "MIMO Systems with Antenna Selection," *IEEE Microwave Magazine*, Volume: 5, Issue: 1, Pages: 46 - 56, March 2004

[13] D.A. Gore, R.U. Nabar and A. Paulraj, "Selecting an Optimal Set of Transmit Antennas for a Low Rank Matrix Channel," ; *IEEE International Conference on Acoustics, Speech, and Signal Processing, 2000. ICASSP '00. Proceedings. 2000*, Volume: 5, Pages: 2785 - 2788, June 2000

[14] S. Sandhu, R.U. Nabar, D.A. Gore and A. Paulraj, "Near-Optimal Selection of Transmit Antennas for a MIMO Channel Based on Shannon Capacity," *Conference Record of the Thirty-Fourth Asilomar Conference on Signals, Systems and Computers, 2000*, Volume: 1, Pages: 567 - 571, Oct. 2000

[15] R.W. Heath Jr., S. Sandhu and A. Paulraj, "Antenna Selection for Spatial Multiplexing Systems with Linear Receivers," *IEEE Communications Letters*, Volume: 5, Issue: 4, Pages: 142 - 144, April 2001

[16] D.A. Gore and A.J. Paulraj, "Mimo Antenna Subset Selection with Space-Time Coding ," *IEEE Transactions on Signal Processing*, Volume: 50, Issue: 10, Pages: 2580 - 2588, Oct. 2002

[17] B. Badic, M.Rupp, H. Weinrichter, "Extended Alamouti Codes in Correlated Channels Using Partial Feedback," *IEEE International Conference on Communications 2004*, Volume: 2, Pages: 896 - 900, June 2004

[18] W.C. Jakes, *Microwave Mobile Communications*, Wiley-Interscience, 1974

[19] J.G. Proakis, *Digital Communications*, McGraw-Hill, 1983

[20] Kai Yu, M. Bengtsson, B. Ottersten, D. McNamara, P. Karlsson and M. Beach, "Modeling of Wide-Band MIMO Radio Channels Based on NLoS Indoor Measurements," *IEEE Transactions on Vehicular Technology*, Volume: 53, Issue: 3, Pages: 655 - 665, May 2004

[21] H. Özcelik, M. Herdin, W. Weichselberger, J. Wallace and E. Bonek, "Deficiencies of 'Kronecker' MIMO Radio Channel Model," *Electronics Letters* , Volume: 39, Issue: 16, Pages: 1209 - 1210, Aug. 2003

[22] Pedersen, K.I.; J.B. Andersen, J.P. Kermoal and P. Mogensen, "A Stochastic Multiple-Input-Multiple-Output Radio Channel Model for Evaluation of Space-Time Coding Algorithms," *IEEE VTS-Fall VTC 2000 52nd Vehicular Technology Conference*, Volume: 2, Pages: 893 - 897, Sept. 2000

[23] H. Weinrichter and F. Hlawatsch, *Stochastische Grundlagen nachrichtentechnischer Signale*, Springer, 1991

[24] S.M Alamouti, "A Simple Transmit Diversity Technique for Wireless Communications," *IEEE Journal on Selected Areas in Communications*, Volume: 16, Issue: 8, Pages: 1451 - 1458, Oct. 1998

[25] H. Jafarkhani, "A Quasi-Orthogonal Space-Time Block Code," *IEEE Transactions on Communications*, Volume: 49, Issue: 1, Pages: 1 - 4, Jan. 2001

[26] M. Rupp and C.F. Mecklenbräuker, "On Extended Alamouti Schemes for Space-Time Coding," *The 5th International Symposium onWireless Personal Multimedia Communications, 2002* , Volume: 1, Pages: 115 - 119, Oct. 2002